ELSEVIER

Contents lists available at ScienceDirect

Journal of Hydrology

journal homepage: www.elsevier.com/locate/jhydrol

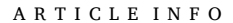


Research papers

Effects of stormwater infrastructure data completeness and model resolution on urban flood modeling

Ashish Shrestha*, Giuseppe Mascaro, Margaret Garcia

School of Sustainable Engineering and the Built Environment, Arizona State University, Tempe, AZ 85281, United States



This manuscript was handled by Marco Borga, Editor-in-Chief, with the assistance of Stefano Orlandini, Associate Editor

Keywords: Urban flood Urban stormwater Hydrodynamic modeling SWMM Urban infrastructure Sampling algorithm

ABSTRACT

The accuracy of hydrologic and hydrodynamic models, used to study urban hydrology and predict urban flooding, depends on the availability of high-resolution terrain and infrastructure data. Unfortunately, cities often do not have or cannot release complete infrastructure data, and high-resolution terrain data products are not available everywhere. In this study, we quantify how the accuracy and precision of urban hydrologichydrodynamic models vary as a function of data completeness and model resolution. For this aim, we apply the one-dimensional (1D) and coupled one- and two-dimensional (1D-2D) versions of the U.S. Environmental Protection Agency's Storm Water Management Model (SWMM) in an urban catchment in the city of Phoenix, Arizona. Here, we have collected detailed infrastructure data, a high-resolution 0.3-m LiDAR-based digital elevation model, and catchment properties data. We tested several model configurations assuming different levels of (i) availability of stormwater infrastructure data (ranging from 5% to 75% of attribute-values missing) and (ii) terrain aggregation (i.e., 4.6 m and 9.7 m). These configurations were generated through random Monte Carlo sampling for SWMM 1D and selective sampling with four cases for SWMM 1D-2D. We ran simulations under the 50-year return period design storm and compared simulated flood metrics assuming the highestresolution and complete data model configuration as a reference. The study found that the model may over or underestimate flood volume and duration with different levels of missing data depending on the parameters roughness, diameter or depth, and that model performance is more sensitive to missing data that is downstream and closer to the outfall as opposed to missing data upstream. Errors in flood depth, area and volume estimation are functions of both the data completeness and model resolution. Missing feature data leads to overestimation of flood depth, while lower model resolution results in underestimating flood depth and overestimating flood extent and volume.

1. Introduction

Urban flooding is a natural hazard impacting public health, environmental quality and the economy (Rahmati et al., 2020). Although the national-level economic and social costs of urban flooding in the U.S. are not routinely recorded, past flood events have resulted in significant property damage and casualties (The National Academy Press, 2019; University of Maryland and Texas A&M University, 2018). For example, urban flooding in Cook County, Illinois resulted in flood losses at a cost of \$660 million between 2007 and 2011 (Festing et al., 2014). Additionally, a 1000-year rainfall event in Ellicott City, Maryland in May 2018 caused over one billion dollars in damages, and heavy rainfall in the metropolitan Detroit area in August 2014 resulted in over \$1.8 billion in damages (University of Maryland and Texas A&M University,

2018). Damages of urban flooding have been also documented outside of U.S., including in Copenhagen, Denmark in July 2011; Catania, Italy in October 2018 (Prokić et al., 2019); Chennai, India in November and December 2015 (Nithila Devi et al., 2019); Ho Chi Minh, Vietnam in November 2018 (Leitold et al., 2021); Beijing, China in July 2012 (Jiang et al., 2018); and Nagoya City, Japan in Autumn 2020 (Tanaka et al., 2020).

Unfortunately, the risk of urban flooding will likely increase world-wide because of intense urbanization and climate change. Urban growth results in a conversion of natural land into impervious areas, which in turn increases runoff and reduces infiltration if proper drainage systems are not put in place. Global warming will likely lead to more intense and frequent extreme precipitation (Farris et al., 2021; Jung et al., 2011; Moftakhari et al., 2015; Wehner et al., 2017; Zhang et al., 2018). Climate

E-mail address: ashres15@asu.edu (A. Shrestha).

^{*} Corresponding author.

projections for the U.S. estimate that the intensity of the heaviest 1% of precipitation events will likely rise across most regions under both intermediate and worst-case climate change scenarios of Representative Concentration Pathway (RCP) 4.5 and RCP 8.5, with the highest projected increase of 40% by 2100 (compared to 1986–2015) under RCP 8.5 in Midwest and Northeast (The National Academy Press, 2019).

One of the major flood-generating mechanisms in cities is pluvial flooding, which occurs when the precipitation intensity exceeds infiltration rate and drainage capacity (Rosenzweig et al., 2018). Pluvial flooding is particularly impactful in urban areas because of the lower threshold for runoff generation and the shorter time of concentration. This flood mechanism has received less attention compared to fluvial or coastal flooding (Rosenzweig et al., 2018). For example, the Federal Emergency Management Agency's (FEMA's) flood hazard analysis and mapping focus only on riverine and coastal flooding (The National Academy Press, 2019). In a study by the First Street Foundation (2020), which included pluvial flooding among other flooding mechanisms, the number of properties across the U.S. with substantial flood risk (defined as inundation>1 cm during 1 in 100 year flood) was found to be 1.7 times FEMA's estimate, confirming the importance of pluvial flooding. In the U.K., it has been estimated that damages from urban pluvial flooding in 2008 exceeded \$0.36 billion, which is a lower cost than the \$0.8-\$2.8 billion calculated for fluvial and coastal flooding; however, future projections indicate that losses due to urban flooding will become similar to or higher than those of other flooding types by 2080 (Dawson et al., 2008; Hall et al., 2005).

The simulation of pluvial flooding requires capturing a range of hydrologic and hydraulic processes, including rainfall-runoff transformation, overland flow routing, and pipe flows. For this aim, hydrologic models with different levels of sophistication have been coupled to hydraulic models simulating water flow in the drainage networks and on the land surface (Guo et al., 2020; Leandro et al., 2009; Noh et al., 2018; Seyoum et al., 2012; Vojinovic and Tutulic, 2009). A key requirement to increase the predictive skill of these coupled hydrologic-hydraulic models is to incorporate small-scale heterogeneities of terrain and stormwater infrastructure into the simulations (Fewtrell et al., 2008; Gallegos et al., 2009). This is because the impacts of pluvial flooding vary significantly at small spatial scales. For example, six inches of moving floodwater can knock down a pedestrian and cause vehicles to loose traction (National Weather Service [NWS], n.d.); in urban areas, where topography is highly heterogeneous, such changes in elevation can happen over short distances. While recent advances have been made towards model improvement and coupling (Cantone and Schmidt, 2011; Chang et al., 2015; Henonin et al., 2013; Leandro and Martins, 2016; Nanía et al., 2015; Wu et al., 2018), the sources of errors in simulations of urban flooding have not yet been fully explored because of uncertainty and limited availability of geospatial data (terrain, soil, land cover, and infrastructure) and high-resolution precipitation forcing required to setup and run the simulations.

Of particular importance to increase accuracy of pluvial flooding prediction is the integration of infrastructure and high-resolution terrain data (Association of State Floodplain Managers [ASFPM], 2020). Infrastructure data includes all components of built stormwater systems, such as catch basins, manholes, conduits, detention and storage basins, drywells and outfalls, whereas terrain data includes urban features such as buildings, street curbs, overpasses and bridges. Unfortunately, these datasets are often incomplete or of poor quality and data collection efforts are resource intensive. Important characteristics of such spatial data quality are completeness, accuracy, consistency and current-ness (Fox et al., 1994; Veregin, 1999). Data completeness as defined by Fox et al. (1994) is the degree to which a data collection has values for all the attributes of all the features. Guptill and Morrison (1995) and Veregin (1999) further characterize data completeness as feature completeness, attribute completeness and value completeness. For example, in a stormwater database, features include components like conduits, catch basins, and manholes; each feature has attributes, such as material or

diameter for conduits; and attributes have numerical or categorical values. In a complete stormwater database, all the system components as features; and its attributes and values are present.

Model development is also challenged by the limited availability of high-resolution spatial data (e.g., 1-m digital elevation models or DEMs), and the need to balance computational cost with accuracy requirements. The resolutions of commonly available DEMs (e.g., 10 m in U.S. (United States Geological Survey [USGS], n.d.)) do not sufficiently capture fine details of urban infrastructure features such as walls, curbs, steps and storm drains, thus preventing the simulation of overland flow in complex urban environments (Fewtrell et al., 2008; Krebs et al., 2014; Leitão et al., 2016; Sampson et al., 2012). Past studies have cautioned that the ideal spatial resolution is between 2 and 5 m for the effective representation of urban features (Arrighi and Campo, 2019; Dottori et al., 2013). The advent of airborne Light Detection and Ranging (LiDAR) has increased the availability of high-resolution (less than 1 m) topographic data that would allow incorporating small-scale heterogeneities found in urban basins into hydrologic models (Bates et al., 2003; Bermúdez and Zischg, 2018; Fewtrell et al., 2011; Noh et al., 2018; Sampson et al., 2012). Despite this promising capability, LiDAR products are available at limited sites, are expensive to acquire, and require significant computational resources to be processed and used in numerical models. More insight is then needed to weigh costs and benefits of investment in LiDAR for urban flood modeling.

Previous studies have evaluated the impacts of simplifying the model representation of certain elements (Krebs et al., 2014), and prior research demonstrates that select aggregation may have limited impacts on model results. For example, Elliot et al. (2009) assessed different aggregations of detention tanks and bioretention, as well as their associated catchment areas, finding that there is little effect on predictions of mean flow, baseflow and water quality at the outlet. However, while aggregation of stormwater control features allows modeling water balance or outflow hydrograph at a lower computational cost, this approach provides limited information on location, duration, and extent of the flood, which is crucial when modeling the impacts of pluvial flooding. Thus, additional research is needed to assess the feasibility of aggregation for spatially distributed street flooding estimation.

As hydrologic-hydraulic models for urban flood modeling are critical to flood prediction, infrastructure design, and adaptation planning, it is crucial to also understand the impact of different sources of error and uncertainty (Pathak et al., 2015). For engineers and planners developing asset management plans (Harvey et al., 2017), designing flood mitigation infrastructure (Kabisch et al., 2017; Kurigi and Hysa, 2021) or rehabilitating drainage structures (Martínez et al., 2018), accurate hydraulic information of the drainage system as well as communication of output uncertainty is vital. Several past studies on different catchment scales focused on, (1) quantifying the rainfall error uncertainty on hydrologic model outputs arising from temporal resolution (Lyu et al., 2018), data products such as satellite rainfall (Bitew and Gebremichael, 2011) or radar rainfall error propagation (Hjelmstad et al., 2021; Sharif et al., 2002); (2) quantifying effect of DEM resolution on urban flood modeling (Leitão et al., 2009; Leitão and de Sousa, 2018). However, little is known about modeling errors arising from missing infrastructure data (e.g., missing features or components) or properties of these features (e.g., missing attributes), and standard approaches on how to deal with data gaps are nonexistent. Further, the effect of DEM and model resolution in conjugation with completeness of infrastructure features in coupled 1D-2D model is not fully understood or quantified.

This study aims at addressing two research questions motivated by the challenges in pluvial urban flood modeling described above, including: (1) How do the proportion and spatial distribution of infrastructure data gaps impact model performance? and (2) How does the spatial resolution of the terrain data interact with infrastructure data gaps to impact the model performance? Model performance is defined as accuracy and precision in modeling flood flow rate, volume, duration, and extent. To examine these research questions, we simulated pluvial

flooding in an urban catchment in the city of Phoenix, Arizona using a semi-distributed, coupled hydrological-hydraulic model based on the U. S. Environmental Protection Agency's (EPA) Storm Water Management Model. We first explored the effect of missing data (i.e., attribute–value of parameters) using the one-dimensional rainfall-runoff and pipe flow model (SWMM 1D). We then examined the combined effect of model resolution (i.e., high and low model resolution) and data completeness (i.e., missing stormwater features) using the coupled 1D-2D model version (SWMM 1D-2D). In sum, our objectives are to assess model error, bias and uncertainty arising from missing infrastructure attribute data; and to investigate the combined effect of infrastructure feature data gaps and coarsening model resolution.

2. Study area, data collection and processing

To answer our research questions, we focus on an urban catchment in the city of Phoenix, Arizona, since the city faces periodic pluvial floods and the required infrastructure data are complete and accessible (Fig. 1a). Phoenix is the capital of the state and the main city of one of the largest metropolitan regions in the U.S., with a population of approximately 4.5 million people. It is in central Arizona and the northeastern Sonoran Desert, downstream of the confluence between the Salt and Verde Rivers. According to the Köppen classification, the climate is hot desert or arid (BWh) with extreme hot summers and mild short winters. The average yearly precipitation is 204 mm, while the mean temperature is 24 °C (Mascaro, 2017). Climate is characterized by

two main seasons that influence the rainfall regime. The first includes a summer period from July to September that is dominated by the North American Monsoon, when convective activity leads to diurnally modulated, localized thunderstorms with short durations (less than 1h) and high rain intensity (Balling and Brazel, 1986). The second season, which ranges from late October through March, is dry and occasionally interrupted by cold fronts, causing widespread storm systems with low-to-moderate rainfall intensity and relatively longer durations of up to a few days (Sheppard et al., 2002). Monsoonal thunderstorms cause severe flash flood events in the region, though other storm types can also trigger flooding. For example, in September 2014 the remnants of Hurricane Norbert triggered pluvial flooding, inundating major roadways throughout the valley (NWS, 2014).

In central Arizona, the spatial variability of annual, seasonal and extreme rainfall is moderately to significantly controlled by terrain, which varies from 220 to 2,325 m above mean sea level (MSL) (Mascaro, 2020, 2018, 2017). The topography of Phoenix is generally flat. The urban form is characterized by a street pattern running in precise grids, and such is the stormwater infrastructure layout. Our study catchment has a total area of 2.4 km². The catchment runoff drains to the south of the main outfall into the Salt River (Fig. 1b). The soil type distribution in the study catchment is presented in Table S1. The weighted average imperviousness relative to the discretized sub-catchments' area is 71.24% while maximum is 99% (Table S2).

The summary of data used in this study is shown in Table 1 and Fig. 2. Table 1 classifies data as vector, raster, or point cloud. These data

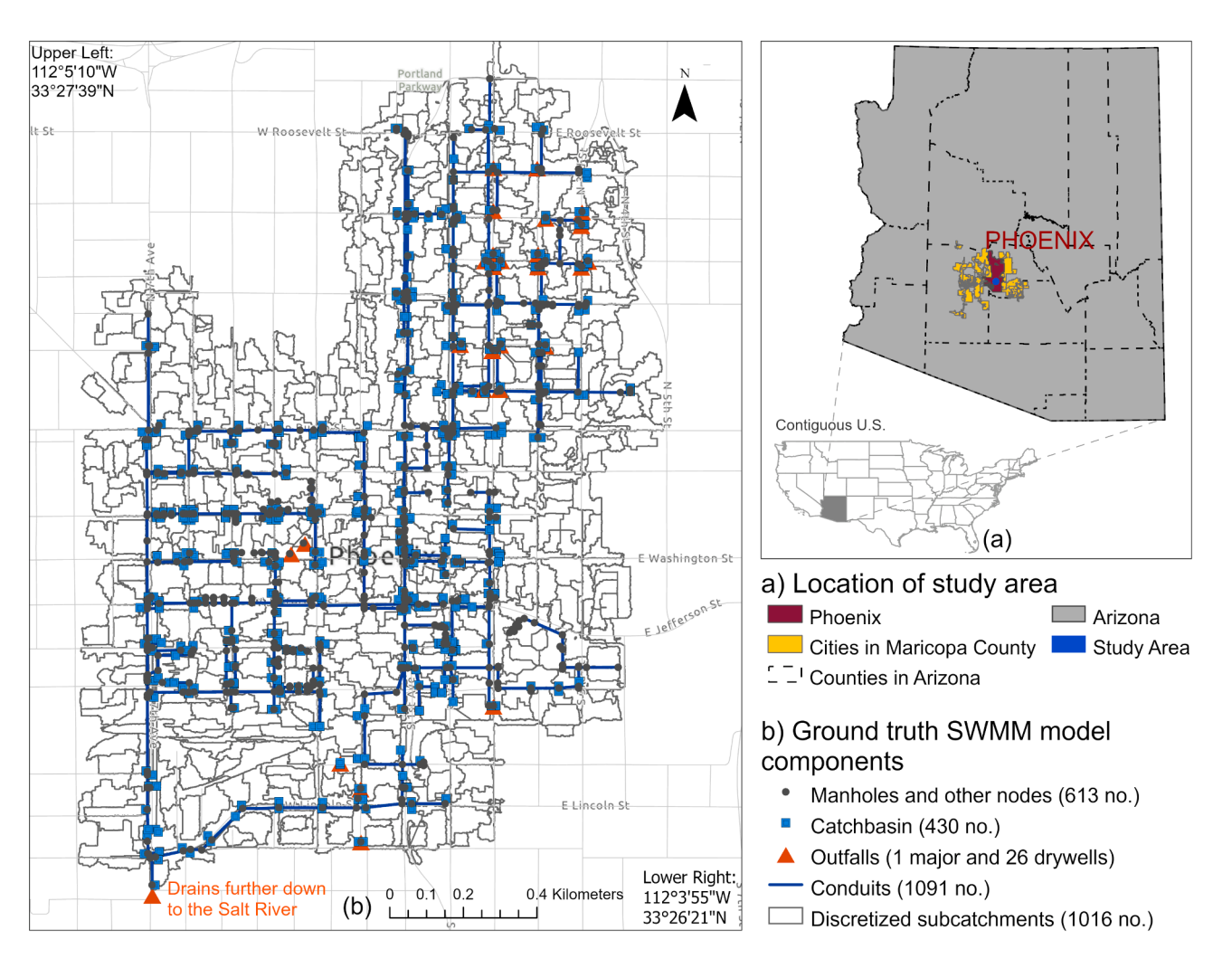


Fig. 1. (a) Location of the City of Phoenix and (b) study catchment with complete stormwater infrastructure data (referred to as the ground truth data set).

Table 1
Data used in this study.

	, -	
Data	Data type	Source
Stormwater infrastructure data	Vector (Secondary data)	Phoenix Public Works Department and Flood Control District of Maricopa County
LiDAR point cloud data	Point cloud (Raw data)	USGS 3D Elevation Program (USGS, n. d.) and Arizona State University (ASU) Geo Spatial hub database
Digital Elevation Model (DEM)	Raster (Processed data)	LiDAR point cloud dataset (ASU, 2018)
Digital Surface Model (DSM)	Raster (Processed data)	LiDAR point cloud data (ASU, 2018)
Soil types and parameters	Vector (Secondary data)	United States Department of Agriculture - Natural Resources Conservation Service, Web Soil Survey database (USDA-NRCS, n.d.); Arizona Department of Transportation, Highway Drainage Design Manual (ADOT, 2014)
Urban imperviousness data	Raster (Secondary data)	National Land Cover Database, Multi- Resolution Land Characteristics Consortium (MRLC, n.d.)

are either raw, processed by the authors for this study or secondary data obtained from the noted source. Fig. 2 shows the layers of spatial data required to build SWMM 1D-2D models. SWMM 1D model also utilizes the same layers without terrain data layers, namely building and mesh grids.

Stormwater infrastructure data with complete features and attributevalues is critical to build the hydrologic-hydraulic model and simulate catchment behavior. The geodatabase for the infrastructure components in Phoenix is stored and updated at irregular intervals by the Phoenix Public Works Department. We obtained the infrastructure data, which is not publicly available, from the Public Works Department in 2019. To ensure that there are no missing data or inconsistencies in the GIS database, we verified through field visits that surface infrastructure features were properly located. The stormwater infrastructure data for the study catchment includes 430 catch basins to collect stormwater runoff; 613 manholes and other nodes which connect upstream and downstream conduits; 1,091 conduits with attributes of material, year built, depth, slope, shape and size; 26 drywells which infiltrate stormwater and are usually present in flat topography; and 1 major outfall where stormwater drains to the Salt River. The details of stormwater components in our study catchment are shown in Figs. 1b and 2a.

Following the definition of data completeness by Guptill and Morrison (1995) and Veregin (1999), in this study we characterize data

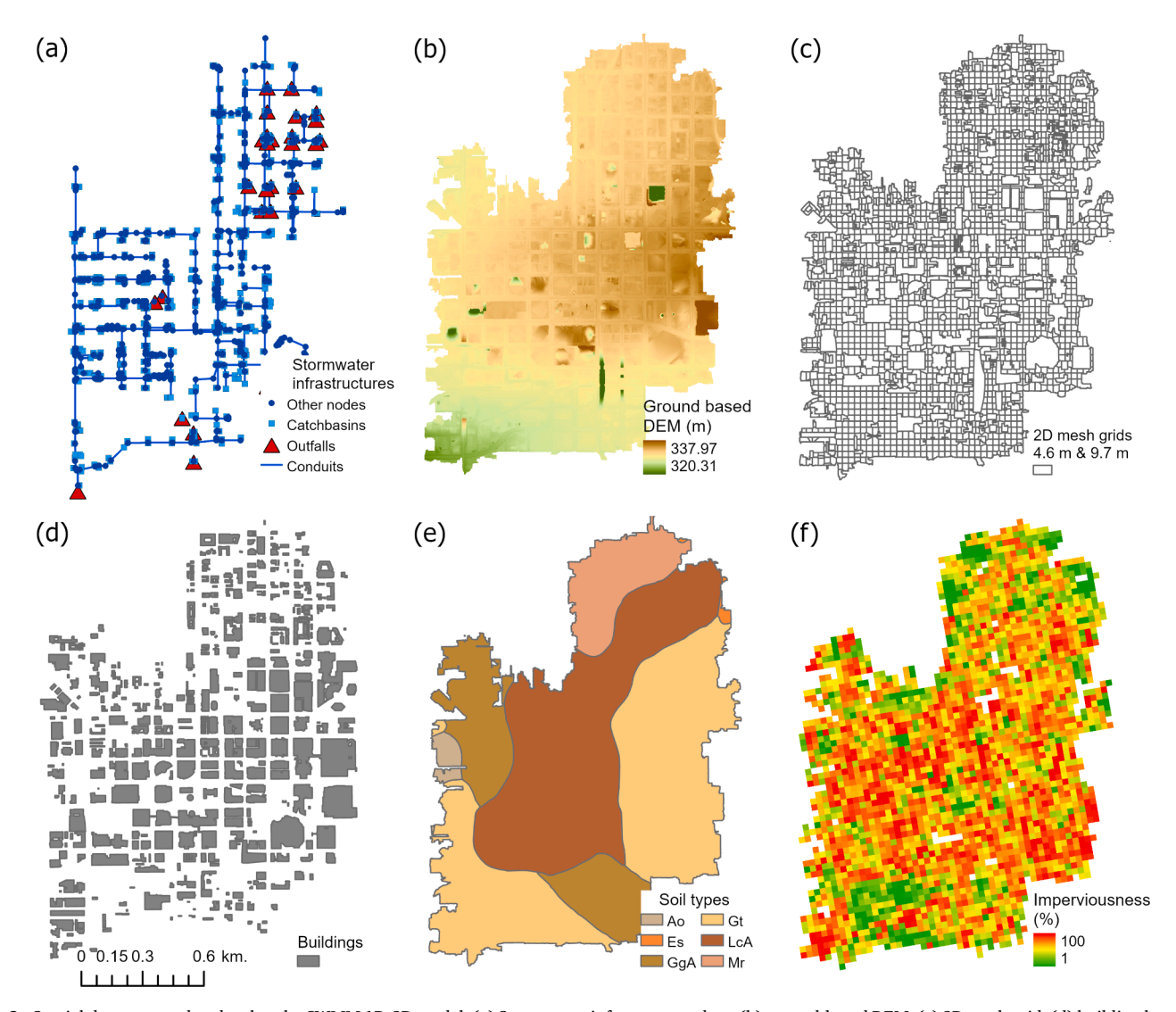


Fig. 2. Spatial data sets used to develop the SWMM 1D-2D model, (a) Stormwater infrastructure data, (b) ground-based DEM, (c) 2D mesh grid, (d) building layer, (e) soil types, and (f) imperviousness.

completeness as feature completeness, which refers to the known presence and location of all stormwater infrastructure components, and attribute-value completeness, which refers to known attributes and values of each component. Accuracy can also be assessed for both features and attribute-values. Feature accuracy refers to whether the feature type and location are correct, while attribute-value accuracy refers to whether infrastructure attributes (e.g., diameter) are correct. This study uses the single most current (and thus consistent) infrastructure dataset; therefore, this analysis does not focus on data consistency nor current-ness. Here, we assume that our field-verified infrastructure dataset is both complete and accurate. We then refer to this infrastructure dataset as the ground truth and the corresponding model built as the ground truth model.

Point cloud LiDAR data were available as a terrain data with 0.3 m spacing for the City of Phoenix (ASU, 2018). Only the point cloud data with return points excluding buildings and vegetations were selected (using the LAS filter and create LAS dataset geoprocessing tool in ArcGIS Pro) to create a ground-based DEM (Fig. 2b) that includes the details of street level and curbs. Since the use of the 0.3-m resolution DEM is computationally too intensive for 2D overland flow computations, a 4.6-m resolution DEM was also generated to create the 2D model (Fig. 2c). In addition to the DEMs, we created a 0.3-m Digital Surface Model (DSM) that includes buildings (Fig. 2d) but not trees (as trees do not impede water flow throughout their full canopy area) in order to delineate the watershed. The buildings act as an impermeable obstruction layer in SWMM 1D-2D model.

Data on the catchment soil types and properties (e.g., suction head, saturated hydraulic conductivity; Fig. 2e) were obtained from the Arizona Department of Transportation (ADOT, 2014). Urban imperviousness data from 2016 with a resolution of 30 m was used as seen in Fig. 2f (MRLC, n.d.). The time series of design storm for a 1/50 annual exceedance probability with 45-min duration and 5-min intervals was created from National Oceanic and Atmospheric Administration (NOAA) Atlas 14 point precipitation frequency estimates (NOAA/NWS, n.d.) using an alternating block method (Chow et al., 1998). This study primarily focuses on extreme flood estimation rather than infrastructure design; thus, a higher return period was chosen. This design storm was used as the input for all simulations. We selected a storm duration of 45 min equivalent to the time of concentration for the catchment.

3. Methodology

In the following sections we describe the development of the semi-distributed hydrologic-hydraulic model using 1D and coupled 1D-2D approaches. We then present the algorithm to fill attribute—value data gaps and the Monte Carlo sampling approach for attribute—value completeness. Lastly, we describe the selective sampling approach to assess the combined effect of feature completeness and model resolution.

3.1. Hydrologic-hydraulic model

We used the U.S. EPA's SWMM version 5.1 (1D model) and Computational Hydraulics International (CHI's) PCSWMM version 7.3.3095 (coupled 1D-2D model). To execute the model and facilitate Monte Carlo sampling, we used the R package 'swmmr' version 0.9.1 (Leutnant et al., 2019). SWMM is a hydrologic-hydraulic modeling tool that simulates rainfall-runoff and routing processes for single precipitation events or in a continuous fashion in urban or rural catchments. It estimates two main processes: i) runoff, which is computed on a collection of discretized sub-catchments that generate runoff and pollutants due to precipitation; and ii) routing, which is the transport of runoff across an underground network of conduits, overland channels and other components. SWMM is a semi-distributed model, and it accounts for various hydrologic processes such as time-varying rainfall, evaporation from standing water, rainfall interception in depression

storage, infiltration into unsaturated soil layers, percolation into groundwater layers, interflow between groundwater and the drainage system, non-linear reservoir routing of overland flow and stormwater capture by low impact development. The details about theoretical background, equations, variables, features and capabilities of SWMM can be found in Rossman (2017) and James et al. (2010).

In this study, we apply two implementations of SWMM: 1) a onedimensional drainage model (SWMM 1D) and 2) a coupled 1D-2D model (SWMM 1D-2D) that adds two-dimensional routing of overland flow of floodwaters. We used SWMM 1D to test the effect of infrastructure data attribute-value completeness. The 1D model was chosen for its faster computation time compared to the coupled 1D-2D model and the ability to execute the model from the source code, which enables Monte Carlo sampling. SWMM 1D-2D was used to assess the combined effects of data feature completeness and model resolution. In practice, a large spatial infrastructure data set is rarely 100 percent complete due to manual data entry error, compilation error and antiquated data as new construction or rehabilitation takes place. However, for this study we assume that the data we acquired from the Phoenix Public Works Department and verified by walk-through surveys are 100 percent complete and accurate. We define this data as the ground truth, where all the required features and attribute-values are complete and accurate. The ground truth model, built from this data and the highest feasible resolution of DEM, serves as the basis for comparing simulations described in the next section.

The hydrologic component of SWMM simulates the rainfall-runoff transformation, after accounting for losses, through a non-linear reservoir model, where the reservoir capacity is maximum depression storage. In this model, the study area catchment is discretized into subcatchments to reflect the spatial heterogeneity in topography, drainage pathway, land cover and soil characteristics that impact rainfall-runoff. We utilized the 0.3-m DSM, consisting of street profiles, buildings and general topography, to delineate the watershed and discretize it into smaller sub-catchments with an average area of 2,428 m² using the watershed delineation tools of PCSWMM. The hydrologic model input is precipitation, and the output from each sub-catchment are surface runoff and losses due to infiltration and evaporation. Surface runoff is defined as the excess volume above the depression storage, which considers the initial abstraction such as surface ponding, interception by flat roofs, vegetation and surface wetting, which eventually evaporates or infiltrates following the storm. Depression storages of 1.25 mm for impervious surfaces and 2.5 mm for pervious surfaces, as suggested by the American Society of Civil Engineers (1992), were assigned for each sub-catchment. To calculate losses due to infiltration, we selected the Green-Ampt infiltration model implemented in SWMM with parameters derived from soil types (ADOT, 2014) which are presented in Table S1. Here, discrete event simulation for the 50-year return period, 45-min design storm for downtown Phoenix (NOAA/NWS, n.d.) is applied to force all of the models. We assumed a constant evaporation rate of 0.76 cm/day (Western Regional Climate Center [WRCC], n.d.) corresponding to the average during monsoon season. The parameters used for the stormwater system are summarized in Table S3. The governing equations and additional details for the hydrologic processes as employed in the SWMM can be found in Rossman (2017) and James et al. (2010).

The hydraulic component of SWMM uses the dynamic wave routine that solves unsteady flow through the network of conduits and nodes, using the conservation of mass and momentum equations. Dynamic wave routing solves the complete one-dimensional Saint-Venant flow equations, whose details can be found in Rossman (2006), which account for channel storage, backwater effects, entrance/exit losses and pressurized flow. Flooding in the system occurs when the hydraulic grade line at a node exceeds the threshold of available depth (i.e., rim elevation). The flooded water in SWMM 1D is accounted as flooding losses which will not re-enter the drainage network unless ponding is allowed. The surcharge depth for manholes was assigned as 0.4 m which

is equivalent to the resistance of manhole lid cover weight. The parameters for the sub-catchments and infrastructure are extracted directly from the attribute-values in the infrastructure database, soil data or DEM. These parameters include rim elevation, invert elevation and depth for catch basin and manholes junctions or nodes; roughness, length, diameter, cross-section and slope for conduits; invert elevation for outfalls and drywells nodes; and area, slope, imperviousness and Green-Ampt parameters for sub-catchments. The relevant outputs from the hydraulic component include: (1) time series of flooding and flow at all nodes and conduits respectively, (2) flood loss time series (i.e., flow exiting the drainage system when the hydraulic grade line reaches the surface) at all nodes and in aggregate (hereafter, referred to as system flooding), and (3) duration of flooding and surcharge at all nodes. The duration of node flooding is the length of time when the hydraulic grade line is above the rim elevation for a particular node. To maintain numerical stability and remove continuity error, a time step of 1 s was selected for both SWMM 1D and 1D-2D models.

For 1D-2D coupled modeling we used PCSWMM due to its additional capability to simulate overland flood routing and associated flood extent, depth, and duration in two dimensions. This model extends the fully dynamic 1D approach in EPA's SWMM5 to 2D free surface flow using a non-uniform mesh that captures the topography, geometry and built structures. SWMM 2D domain solves SWMM5 dynamic wave routing with or without inertial terms; ignoring inertial terms creates diffusive wave routing, which is virtually indistinguishable from fullterm dynamic wave solution (Finney et al., 2012; James et al., 2013). In the 2D domain, the overland surface is discretized into a square mesh and represents each 2D cell with a 2D node or a junction, where invert elevation for these nodes is assigned the ground surface elevation or rim elevation of adjacent coupled 1D nodes (Finney et al., 2012; James et al., 2013). In the 2D domain of 1D-2D coupled model, grid cells require slope and roughness parameters. SWMM 1D-2D uses the same subcatchment delineation and catchment properties, as well as hydraulic network and hydrologic properties, as described above for SWMM 1D. The catch basin nodes are coupled with 2D mesh cells using orifices in 1D-2D integrated model, such that the volume of water exiting an orifice, when flooding occurs, is routed over the 2D mesh cells. This excess flow can pond on the overland grid cells and re-enter the drainage network when the hydraulic grade subsides below ground elevation.

3.2. Random sampling of infrastructure data

First, we tested the significance of infrastructure data completeness on the model. A one-at-a-time sensitivity analysis was conducted to identify the important infrastructure parameters using a built-in tool available in PCSWMM (Finney and Gharabaghi, 2011). Sensitivity analysis assesses the rate of change in response of the model with respect to changes in the model input parameter and the relative importance of parameters to have more accurate values, as measured by the sensitivity gradients (James, 2003). Details of sensitivity analysis are presented in Section S3 of the supplementary material. We selected five infrastructure-related parameters from stormwater components: conduit diameter, node depth (i.e., maximum distance from invert elevation to rim elevation), conduit roughness, inlet offset (i.e., the distance from a conduit's inlet end to the connected node invert elevation), and outlet offset (i.e., the distance from a conduit's outlet end to the connected node invert elevation). All parameters are sampled uniformly within lower to higher parameter values given by an uncertainty level of 50% as described in Section S3. Out of the five parameters tested, we found that the three most sensitive parameters are conduit roughness, conduit diameter and node depth (hereafter, referred to as roughness, diameter and depth), as shown in Table 2 where larger absolute values of the sensitivity gradient indicates more sensitive parameters.

To test the impact of missing attribute-value data on the model, we developed an algorithm to randomly sample conduits and nodes, remove values of roughness, diameter and depth in these selected

 Table 2

 Sensitivity analysis of infrastructure related parameters.

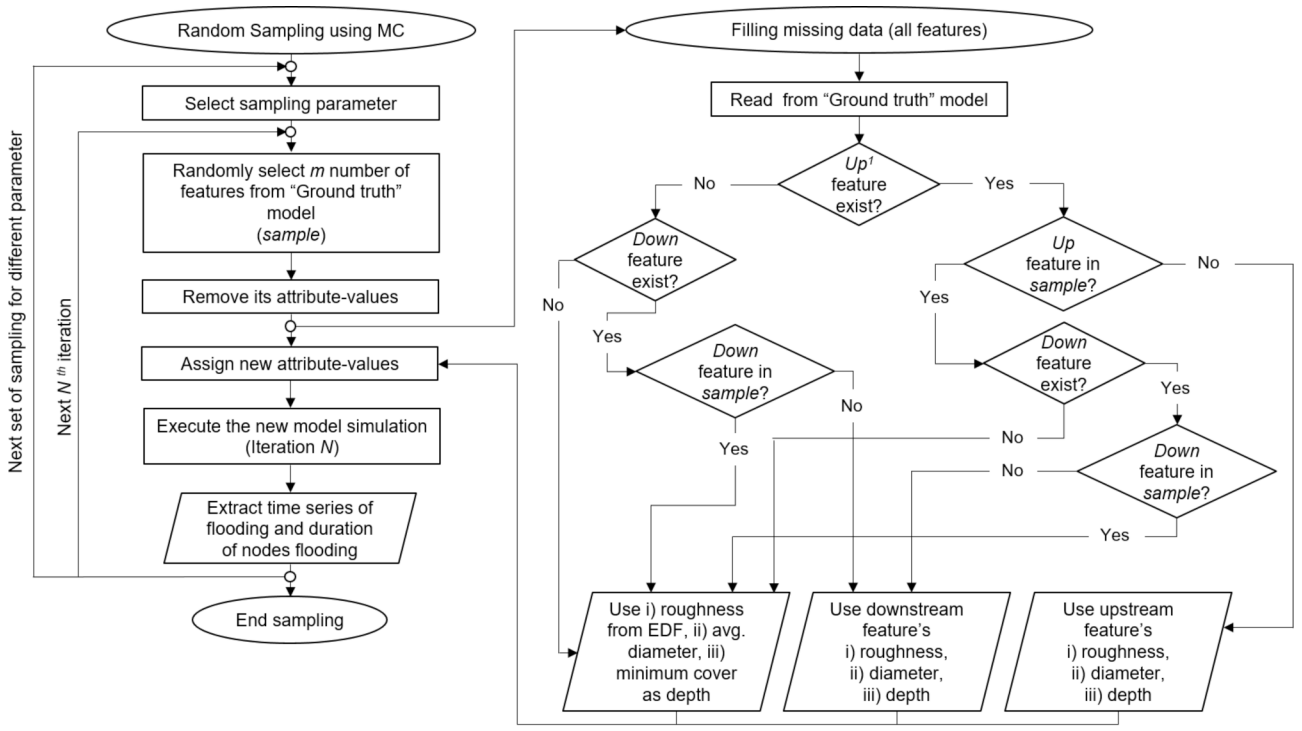
Parameter	Initial parameter value	Mean sensitivity gradient				
Diameter	ground truth	-0.270				
Depth	ground truth	-0.197				
Roughness	ground truth	0.109				
Outlet offset	5 cm	-0.001				
Inlet offset	5 cm	0.000				

features, and estimate these missing attribute-values using the remaining data and design standards. The algorithm enables us to test many combinations of missing attribute-values using Monte Carlo sampling. The replacement component of the algorithm is essential as a SWMM model cannot be run without specifying all parameter values. The replacement criteria for missing attribute-value is implemented in accordance with the available design standards and modeling practice. The detailed process algorithm is described below, and the overall method for random sampling is illustrated in Fig. 3.

The algorithm to sample roughness, diameter and depth, illustrated in Fig. 3, develops and runs a new SWMM 1D model for each iteration N=100 times by randomly removing a specified percentage of each of the three parameters identified above, then filling these gaps based on the remaining information available. The process can be summarized into three main steps:

- 1. Randomly select the number of conduits and nodes corresponding with the percent of missing attribute-values specified (i.e., *m* number of features to be sampled per parameter). For the selected sample, delete existing roughness, diameter, or depth.
- 2. Replace deleted attribute-values with an informed estimate. The estimation algorithm is specific to the parameter:
 - a. Roughness: identify the upstream pipe and apply its roughness. If the upstream roughness attribute is missing, then use the downstream roughness. If both upstream and downstream roughness are missing, randomly sample an empirical distribution function (EDF) of roughness from available information (i.e., conduits with known roughness). The empirical distribution of roughness in the ground truth model is presented in Fig. S2 of the supplementary material (Section S5).
 - b. Diameter: identify the upstream pipe and apply its diameter. If the upstream diameter attribute is missing, then use the downstream diameter. If both upstream and downstream diameters are missing, then use the mean diameter of all conduits in the dataset with known diameters.
 - c. Depth: identify the upstream node and apply its depth. If upstream depth is missing, then use the depth of downstream feature. If both upstream and downstream depths are missing, assume a minimum cover of ~ 0.91 m as per the Arizona drainage design manual (ADOT, 2014). The node depth information is shared by both connected node (or junction) and conduits. Note that there are a few conduits with $\sim 0\%$ slope in the ground truth and randomly sampled models, particularly for shorter length conduits, but the overall slope is positive. In addition, elevation of the street surface and the rim elevations gradually slope downward from upstream to downstream nodes, thus in this particular catchment the negative slopes are avoided when sampling depth.
- 3. Run SWMM 1D and extract the time series of system flooding and duration of flooding (if present) at each node.

Model accuracy is defined relative to the ground truth model output and is quantified by the mean absolute error (MAE) and percent bias (PBIAS). The MAE and PBIAS for system flooding (SF in subscript) are defined as:



Note: 1 Up/Down refers to upstream and downstream

Fig. 3. Overview of the random sampling process.

$$MAE_{SF} = \frac{1}{N} \sum_{j=1}^{N} \left(\frac{1}{T} \sum_{t=1}^{T} |y_{t,j} - x_t| \right)$$
 (1)

$$PBIAS_{SF} = \frac{1}{N} \sum_{j=1}^{N} \left[\frac{\sum_{t=1}^{T} (y_{t,j} - x_t)}{\sum_{t=1}^{T} x_t} \right]$$
 (2)

where, $y_{t,j}$ is the simulated flow at each time steps t (t = 1, ..., T) for the j-th (j = 1, ..., N) iterations (where N = 100), and x_t is the value simulated by the ground truth model. Both MAE_{SF} and PBIAS_{SF} were first computed as the comparison of hydrographs obtained from sampled and ground truth models, and then averaged across all 100 iterations.

For the duration of node flooding, MAE and PBIAS (FD in subscript) were computed from the mean and maximum durations of node flooding in 100 iterations compared to the ground truth, which is defined as:

$$MAE_{FD} = \frac{\sum_{j=1}^{N} |y_j - x_j|}{N}$$
 (3)

$$PBIAS_{FD} = \frac{\sum_{j=1}^{N} (y_j - x_j)}{\sum_{i=1}^{N} x_i} \times 100$$
 (4)

where, y_j is mean (or maximum) duration of node flooding for each j=1 to N^{th} iteration (where N = 100), x_j is the mean (or maximum) duration of node flooding in the ground truth model.

Model uncertainty describes the degree of variation in model output across sampled simulations and is quantified by the relative interquartile range (RIQR), which is defined as:

$$RIQR = \frac{q_{0.75} - q_{0.25}}{q_{0.5}} \times 100 \tag{5}$$

where, $q_{0.75}$, $q_{0.25}$, and $q_{0.5}$ represent upper quartile, lower quartile, and median, respectively, for the empirical distributions of either maximum system flooding (i.e., peak flow) or duration of flooding averaged (or maximum) across all nodes. Precision is referred to as the inverse of uncertainty.

The significance of missing data was tested in terms of the level and

location of missing data. For different levels of missing data (5%, 25%, 50% and 75%), the number of features sampled, m is the corresponding percentage of missing data multiplied by the total number of relevant features (i.e., conduits or nodes). Then, to assess the impact of the location of missing data, we assumed that 50% of data is missing and divided the catchment into two regions, the upstream and downstream. The 50% missing data level was selected because, as shown later in the results, model error increased consistently across parameters with increasing missing data until 50% when sampling the full catchment; beyond 50% the pattern was mixed. The upstream and downstream features were identified by conditional selection of features that are above or below the median distance from the main outfall for the upstream or downstream region, respectively. To test the influence of the location of missing data, the random sampling method described above with the same N = 100 iterations was repeated with the removed attribute-values limited to the upstream and then downstream regions of the network. For random sampling, only the SWMM 1D model was used since the computation time of SWMM 1D-2D is too long to perform many runs. The SWMM 1D-2D model was reserved for selective sampling, as described next.

3.3. Selective sampling

We applied selective sampling of SWMM 1D-2D models to assess the impact of different combinations of feature data completeness and model resolution on model performance. Model resolution for the semi-distributed model is defined in terms of the resolutions of the 2D mesh grid and the DEM utilized to create such a grid. Four selective sampling models were created (Table 3).

In the low-resolution models (HDLM and LDLM), slopes for the discretized sub-catchments were assigned from the coarser-resolution, 9.7-m DEM to account for the fact that high-resolution terrain could not be available in all places and that the most commonly available DEM resolution from USGS is $1/3^{\rm rd}$ arc second (~ 10 m). Although two of the selective sampling models (LDLM and LDHM) have missing features or incomplete infrastructure data, the attribute-values for all remaining

Table 3 Four selective sampling models. Note that HD/LD the first two letters refers to stormwater data (i.e., HD = high data or complete data, LD = low data or incomplete data) and HM/LM refers to model resolution (i.e., HM = high model resolution, LM = Low model resolution).

Sampling model	Details on infrastructure	DEM resolution (m)	2D mesh cell resolution (m)
High infrastructure data completeness and high model resolution (HDHM)	ground truth	0.3	4.6
High infrastructure data completeness and low model resolution (HDLM)	ground truth	9.7	9.7
Low infrastructure data completeness and low model resolution (LDLM)	Incomplete infrastructure model where ~ 50% of the upstream components (features) were missing from the ground truth model (Fig. S1)	9.7	9.7
Low infrastructure data completeness and high model resolution (LDHM)	Incomplete infrastructure model where ~ 50% of the upstream components (features) were missing from the ground truth model (Fig. S1)	0.3	4.6

features are the same as the ground truth. The selective sampling results were compared in terms of flood depth, volume and extent. Flood depth refers to the maximum water level observed in the 2D mesh cells at the time of peak flooding. Flood volume refers to the sum of all flooding fluxes from 1D nodes to 2D grid cells through orifices integrated over the whole flood period. Flood extent refers to the sum of the areas of 2D mesh cells with floodwater > 0 mm at the time of peak flooding.

4. Results and discussion

This section first presents simulation results from Monte Carlo sampling of SWMM 1D model recounting the effects of different levels and locations of incomplete data on modeled peak flood flow and duration. Then, we present SWMM 1D-2D modeling results for four selective sampling models characterized by combinations of complete or incomplete infrastructure data and high or low model resolution, particularly focusing on flood depth, extent and volume.

4.1. Evaluation of random sampling

The impacts of missing attribute-values for the three selected model parameters on the simulated flooding conditions and metrics are summarized in Figs. 4 and 5. Specifically, Fig. 4 shows the distribution of simulated flood duration at all nodes for the three sampled parameters in 100 Monte Carlo sampling and the ground truth model at different percentages of missing attribute-values. Fig. 5 presents boxplots of 100 Monte Carlo sampling for maximum system flooding (Fig. 5a-c), maximum flooding duration (Fig. 5d-f), and average flooding duration (Fig. 5g-i) as a function of percent of missing data (hereafter, PMD). Table 4 reports error and uncertainty metrics as defined in Section 3.2. For the clarity of exposition, these figures and table are discussed in the following three sub-sections focusing separately on sampling roughness, diameter, and depth. Finally, in the last subsection, we illustrate the effect of missing attribute-values at upstream and downstream portions of the basin for PMD = 50% for the three parameters.

4.1.1. Effect of roughness

We begin by discussing Fig. 4, where the distribution of flood

duration simulated by the ground truth model is displayed by a red curve, whereas the ensemble simulations of 100 iterations for different levels of missing data are shown by grey curves. The ground truth model predicts that 564 nodes will be flooded for a varied duration from 0.01 to 1.03 hr, or an overall average duration of 0.21 hr. The density plot for ground truth (Fig. 4) shows the number of flooded nodes decreases rapidly for durations up to 0.2 hr, rises slightly until 0.5 hr, and then decreases at a lower rate up to about 1 hr. When only 5% of the roughness data are missing, the ground truth distribution is well captured across the simulations (Fig. 4a). However, as PMD increases (Fig. 4b-d.), the Monte Carlo runs simulate slightly higher number of nodes that are flooded for 0.01 hr, and slight increase in uncertainty observed between 0.1 and 0.5 hr.

Fig. 5a,d,g and Table 4 show that errors, bias and uncertainty of the simulated flood metrics increase only slightly as PMD of roughness increases. Bias and uncertainty are low but increase for higher PMD, as seen in the peak flooding flow rate (maximum PBIAS of -0.45%, max RIQR of 0.27%), maximum duration (maximum PBIAS of -1%, max RIOR of 2.94%) and average duration (maximum PBIAS of -1.2%, max RIOR of 1.53%). In other words, when the data available on pipe roughness decreases, our algorithm designed to replace missing data results in low error, bias and uncertainty. This is explained in part by algorithm skill and in part by the fact that in the ground truth data the majority (90%) of the conduits are concrete (including reinforced concrete and rubber gasket reinforced concrete pipe, all of which have an average roughness of $0.015 \text{ sec/m}^{1/3}$ as presented in the Fig. S2 of the supplementary material). Given the shape of this empirical distribution the probability of sampling the incorrect roughness is low. Acknowledging that other locations will present a greater challenge for sampling roughness, we investigated how the PMD for roughness would affect the model outputs if the distribution was not dominated by a single conduit material. For this we created a hypothetical set of conduits (using the same model and holding other parameters constant) where distribution of materials is 12% concrete, 51% corrugated metal pipe, and 37% smooth plastic (HDPE or PVC). This distribution is valid per the drainage design standards (City of Phoenix, 2013) (see Section S5 for details). In this hypothetical conduit distribution, we found that error, bias and uncertainty are higher but remain moderate at 50% PMD or lower (PBIAS less than 5%, RIQR less than 10%, Figs. S3-S4 and Table S4). The error associated with different PMD of roughness could be reduced with information on the relationship between pipe age, size and material, if available.

4.1.2. Effect of diameter

The effect of increasing the diameter PMD on the simulated distribution of flood duration is (Fig. 4e-h): (1) lower (higher) number of nodes for durations between 0.01 and 0.3 hr (0.6 and 0.9 hr), (2) equal likelihood of simulating higher or lower number of nodes flooded between 0.3 and 0.5 hr. However, the uncertainty does not increase consistently with PMD. The boxplots of the three flood metrics related to missing diameter data exhibit a nonlinear behavior (Fig. 5b,e,h). The peak system flooding and mean flood duration are overestimated, while maximum flood duration is underestimated. This is because the maximum flood duration tends to occur at the peripheral nodes (connected to 0.3-m diameter pipes) in the network where sub-catchment runoff drains into the network, whose downstream conduit's diameter are usually > 0.3 m. Thus, the current sampling algorithm underestimates peripheral node surcharge and flooding, and the majority of Monte Carlo simulations underestimate maximum flood duration. For all metrics, the largest MAE is obtained for PMD = 50%. The largest PBIAS for peak system flooding and mean flood duration is also obtained for PMD = 50%. The largest uncertainty for peak system flooding is obtained for PMD = 25%, for maximum flood duration is obtained for PMD = 5%, but for mean flood duration is obtained for PMD = 75%while uncertainty range is similar for PMD = 5% to 25% (Table 4). When sampling from PMD = 5% to 50%, error increased for all metrics, but

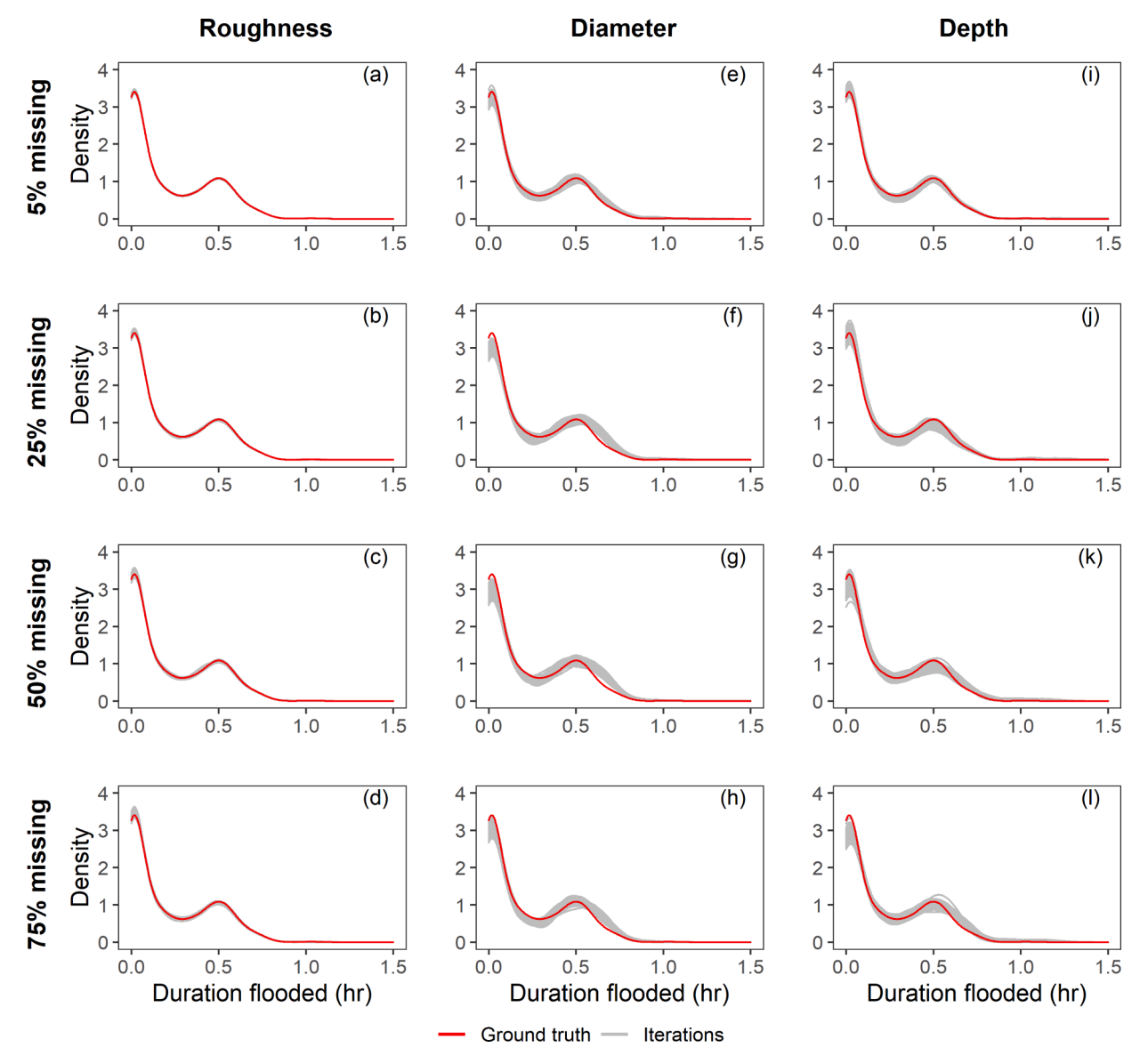


Fig. 4. Monte Carlo sampling results showing distribution of flood duration at all nodes with observed flooding while sampling (a-d) roughness, (e-h) diameter and (i-l) depth at different levels of missing attribute-values. One hundred iterations (grey) are compared with the ground truth model (red). Note: Density plots (Wickham, 2009) are smoothed version of frequency polygon based on kernel smoothers useful to compare shape of the distributions; here, default bandwidth adjustment of 1 and gaussian kernel was selected. (For interpretation of the references to colour in this figure legend, the reader is referred to the web version of this article.)

uncertainty decreased for peak system flooding and maximum flood duration or remained stable for mean flood duration. At PMD = 75%, sampling results showed slight improvement in accuracy as shown by MAE and observed in Fig. 5b,e,h. These outcomes are a consequence of the algorithm adopted to replace missing diameter data. As PMD rises, there are more chances that missing diameters are assigned the average diameter of the stormwater system (see Fig. 3), so that several peripheral pipes (trunk pipes) in the network are oversized (undersized). In the ground truth model, 68.7% of conduits are circular 0.3-m pipes, but the average is 0.46 m. The average and median diameter are similar in this case, and both result in the selection of the same standard conduit size (0.46 m or 18 in.). Overestimating small pipes reduces the risk of stormwater capacity constraints and surcharge in the periphery of the network, which explains decrease in maximum system flooding and duration of flooding. In contrast, underestimating large pipes leads to increased probability of surcharge along the main conduit, which can also lead to surcharge in upstream peripheral conduits. It is also important to note that maximum flooding duration does not signify

maximum flood flow rate or volume, just the longest duration.

4.1.3. Effect of depth

The effect of missing depth on the simulated distribution of flood duration is that when PMD = 5%, the model simulated more flooded nodes between 0.01 and 0.1 hr but lower between 0.2 and 0.5 hr (Fig. 4i). While at PMD = 25%, the model is equally likely to simulate higher or lower number of nodes that will be flooding between 0.01 and 0.1 hr, while it mostly simulates lower number of nodes flooded between 0.2 and 0.7 hr (Fig. 4j). When PMD = 50% or 75%, the model simulates lower number of nodes flooded between 0.01 and 0.1 hr, it is equally likely to simulate higher or lower number of nodes flooded between 0.1 and 0.5 hr, but more likely the model simulates higher number of nodes flooded between 0.5 and 0.9 hr (Fig. 4k-l). Error in estimating peak system flooding and average duration of nodes flooding (as shown by MAE and PBIAS) increases monotonically with increasing PMD, with the largest error occurring at PMD = 75% (Fig. 5c,i). Lowest precision (or highest uncertainty) occurs at different PMD for different metrics

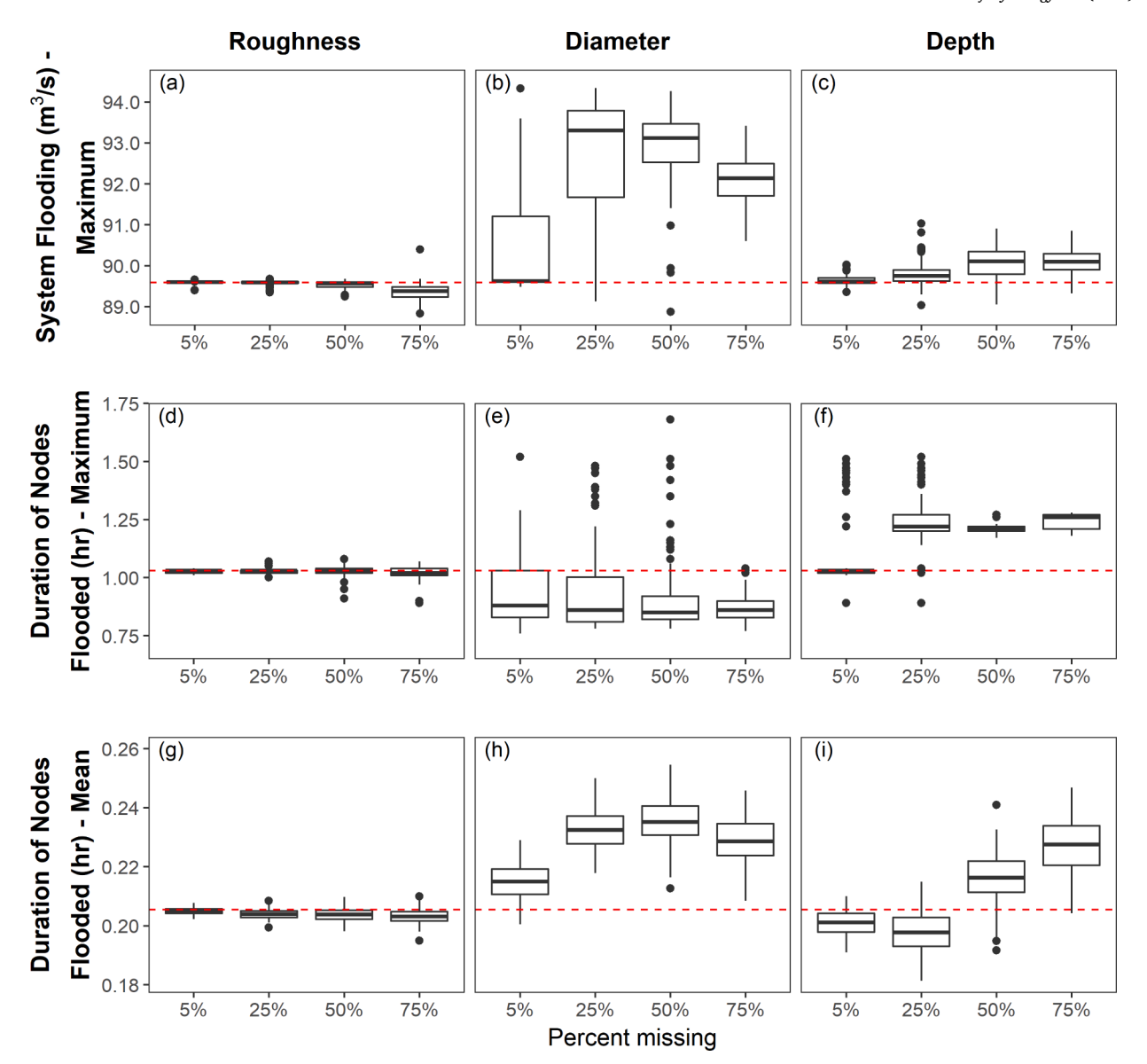


Fig. 5. Monte Carlo sampling results showing (a-c) maximum system flooding, (d-f) maximum duration of nodes flooding, and (g-i) average duration of nodes flooding with different percentages of missing sampling roughness, diameter or depth data. Boxes represent the 25^{th} , 50^{th} and 75^{th} percentiles and whiskers represent $\pm 1.5 \times IQR$ of the 25^{th} and 75^{th} percentiles. Horizontal red dash lines represent the values simulated by the ground truth model. (For interpretation of the references to colour in this figure legend, the reader is referred to the web version of this article.)

Table 4
System flooding metrics of average of MAE and PBIAS (from ensemble simulations vs. ground truth) and RIQR of peak system flooding; and flood duration metrics of MAE and PBIAS (from the maximum and mean duration of flooding in ensemble simulations vs. ground truth) and RIQR of maximum and mean duration of nodes flooded for random sampling with different percentages of missing attribute-values.

Sampling		System flooding			Flood duration (Maximum)			Flood duration (Mean)		
Attribute	Missing percent (%)	MAE (m ³ /s)	PBIAS (%)	RIQR (%)	MAE (hr)	PBIAS (%)	RIQR (%)	MAE (hr)	PBIAS (%)	RIQR (%)
Roughness	5	0.34	-0.00	0.01	0.00	-0.40	0.97	0.00	-0.30	0.74
	25	0.85	-0.04	0.03	0.01	-0.10	0.97	0.00	-0.70	1.08
	50	1.69	-0.15	0.13	0.01	-0.30	1.94	0.00	-0.90	1.50
	75	3.62	-0.45	0.27	0.02	-1.00	2.94	0.00	-1.20	1.53
Diameter	5	20.48	3.00	1.79	0.15	-9.10	22.73	0.01	4.60	4.00
	25	55.28	9.00	2.26	0.17	-8.80	22.38	0.03	13.20	4.11
	50	62.06	10.14	1.00	0.18	-11.70	11.76	0.03	14.60	4.16
	75	60.84	9.82	0.85	0.16	-15.80	8.43	0.02	11.30	4.46
Depth	5	1.93	0.24	0.13	0.05	4.00	0.97	0.00	-2.00	3.11
	25	9.76	1.54	0.30	0.21	20.60	5.74	0.01	-3.60	4.93
	50	18.76	2.92	0.61	0.18	18.00	1.65	0.01	5.10	4.89
	75	20.79	3.26	0.44	0.21	20.70	4.76	0.02	10.80	5.87

(Table 4). There was an increase in precision for estimating peak system flooding when PMD increased to 75% from 50%, and for estimating maximum flood duration when PMD increased to 50% from 25% (Table 4 and Fig. 5 c,f). At PMD = 5%, the model response does not significantly change in terms of peak system flooding (Fig. 5c) or maximum duration of nodes flooded (Fig. 5f), except the outliers for highest duration of nodes flooded are from few significant nodes being assigned average depth whose upstream and downstream depth are missing. As PMD increased from 50% to 75% for the peak system flooding and from 25% to 75% for maximum duration of node flooding, the model accuracy didn't change much as shown by MAE and PBIAS (Table 4). The model simulates lower mean duration of nodes flooded when PMD is 5% or 25%, and higher when PMD is 50% or 75% (Fig. 5i). This is because when PMD is 5% or 25% it is more likely that upstream or downstream depth is present which either increases the depth or creates uniform slopes, thus improving the capacity of the network causing less surcharge. In contrast when PMD is 50% or 75% it is more likely that both the upstream and downstream depth are missing, thus minimum depths are assigned creating non-homogenous depth. Thus, modelers should be cautious in estimating missing depth.

In sum, this analysis demonstrates how the missing infrastructure attribute-values affects estimation of pluvial flooding under reasonable assumptions for filling missing roughness, diameter and depth based on available information and design standards (as shown in Fig. 3). While estimation could be improved by carefully examining each instance of missing data individually, this is often not feasible due to resource constraints. This estimation method can quickly estimate many missing attribute-values and the specific algorithms can be adjusted to fit local design standards and available information.

4.1.4. Effect of location of missing data

We also examined how model performance is affected by the location of missing data, by assuming PMD = 50% either in the upstream or downstream portion of the network, as described in the methodology. Fig. 6 shows boxplots of flood metrics derived from N=100 Monte Carlo sampling, while metrics values are reported in Table 5. Figure S5 and Table S5 in the supplementary material (Section S5) shows the effect of missing roughness in hypothetical conduit distribution. It is apparent that lack of information in the downstream section leads to higher error, bias, and uncertainty. This means that when missing data is in the

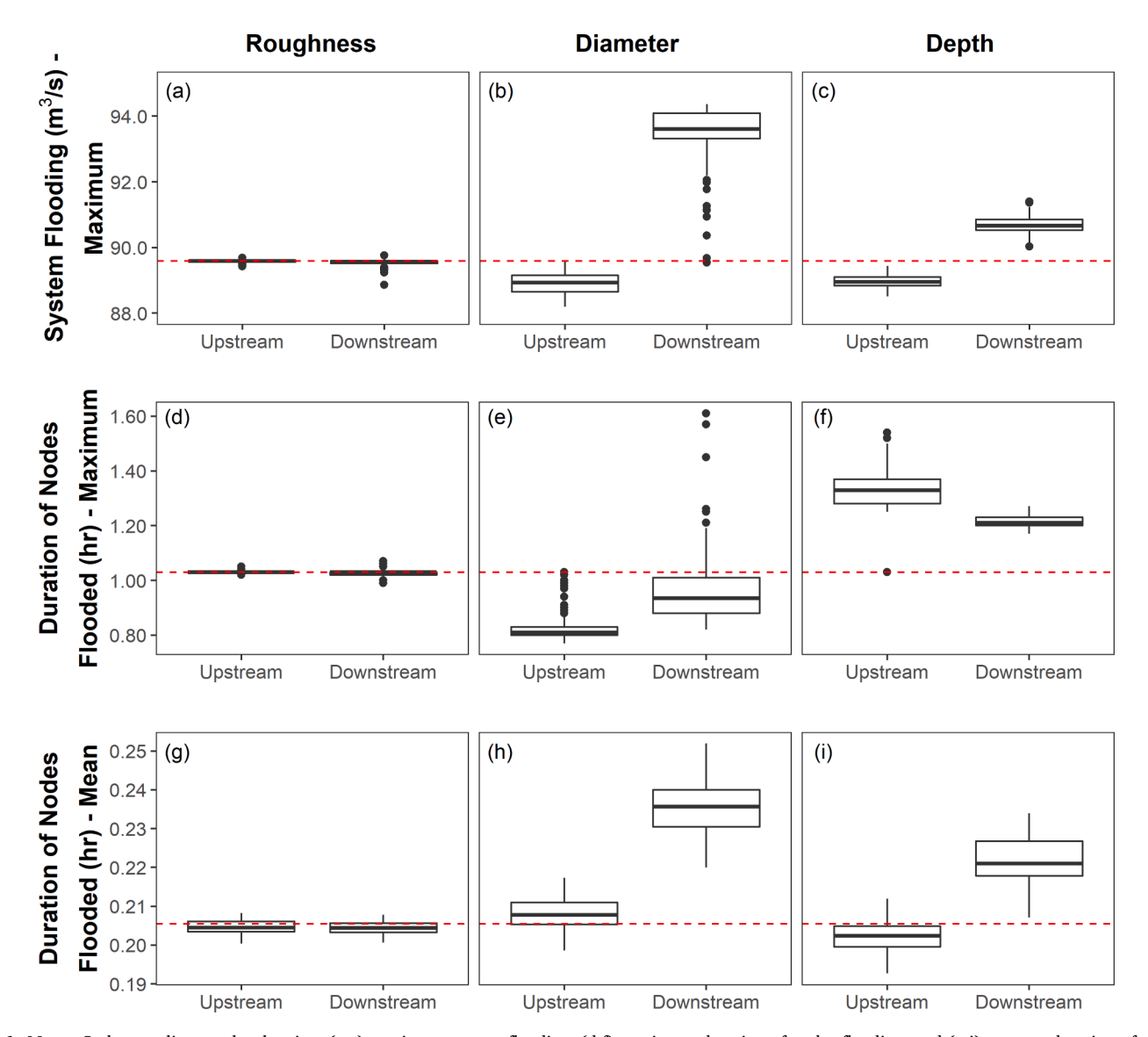


Fig. 6. Monte Carlo sampling results showing, (a-c) maximum system flooding, (d-f) maximum duration of nodes flooding, and (g-i) average duration of nodes flooding while sampling roughness, diameter and depth at 50% PMD from *upstream* versus *downstream* locations. Boxes represent the 25^{th} , 50^{th} and 75^{th} percentiles and whiskers represent $\pm 1.5 \times IQR$ of the 25^{th} and 75^{th} percentiles. Horizontal red dash lines represent the ground truth model. (For interpretation of the references to colour in this figure legend, the reader is referred to the web version of this article.)

Table 5
System flooding metrics of the average MAE and PBIAS (from ensemble simulations vs. ground truth) and RIQR of peak system flooding; and flood duration metrics of MAE and PBIAS (from the mean and maximum durations of flooding in ensemble simulations vs. ground truth) and RIQR of mean and maximum durations of nodes flooded for random sampling of missing locations of attribute-values.

Sampling		System flooding			Flood duration (Maximum)			Flood duration (Mean)		
Attribute	Location of missing data	MAE (m ³ /s)	PBIAS (%)	RIQR (%)	MAE (hr)	PBIAS (%)	RIQR (%)	MAE (hr)	PBIAS (%)	RIQR (%)
Roughness	Upstream	0.87	0.00	0.00	0.00	0.00	0.00	0.00	-0.40	1.20
	Downstream	1.73	-0.10	0.10	0.01	-0.40	1.00	0.00	-0.50	1.10
Diameter	Upstream	7.73	-0.60	0.60	0.2	-19.50	3.70	0.00	1.20	2.70
	Downstream	83.95	10.40	0.80	0.1	-5.50	14.00	0.03	14.50	4.00
Depth	Upstream	5.23	-0.40	0.30	0.3	29.70	6.70	0.00	-1.60	2.60
	Downstream	24.21	2.80	0.40	0.2	18.40	2.50	0.02	8.10	4.00

downstream region of the catchment, the approximation to fill missing data that works for upstream attributes may be insufficient. It also establishes the relative importance of a feature's distance from the outfall, indicating that distance from the outfall might be an important input into a more sophisticated estimation algorithm.

Monte Carlo sampling for the three parameters showed varied degrees of relative importance. Out of the three attributes, missing diameter had the most effect in downstream sampling, as it could lead to the highest error in system flooding and average duration of nodes flooding. Missing diameter in the downstream section led to the lowest model precision, as indicated by a RIQR of 0.8% for system flooding and a RIQR of 14% (and 4%) for maximum (and mean) duration of nodes flooding

(Fig. 6 and Table 5).

4.2. Evaluation of selective sampling

The following section describes the impact of model resolution and infrastructure feature completeness on modeled flood depth, volume and extent. Four cases were modeled, each containing either high (0.3-m DEM and 4.6-m 2D mesh, HM) or low (9.7-m DEM and 9.7-m 2D mesh, LM) resolution and either high (complete information, HD) or low (50% of upstream features missing, LD) infrastructure data (see Table 3). To visualize differences across the domains, changes in DEM resolution resulted in changes in the slope of discretized catchments, as shown in

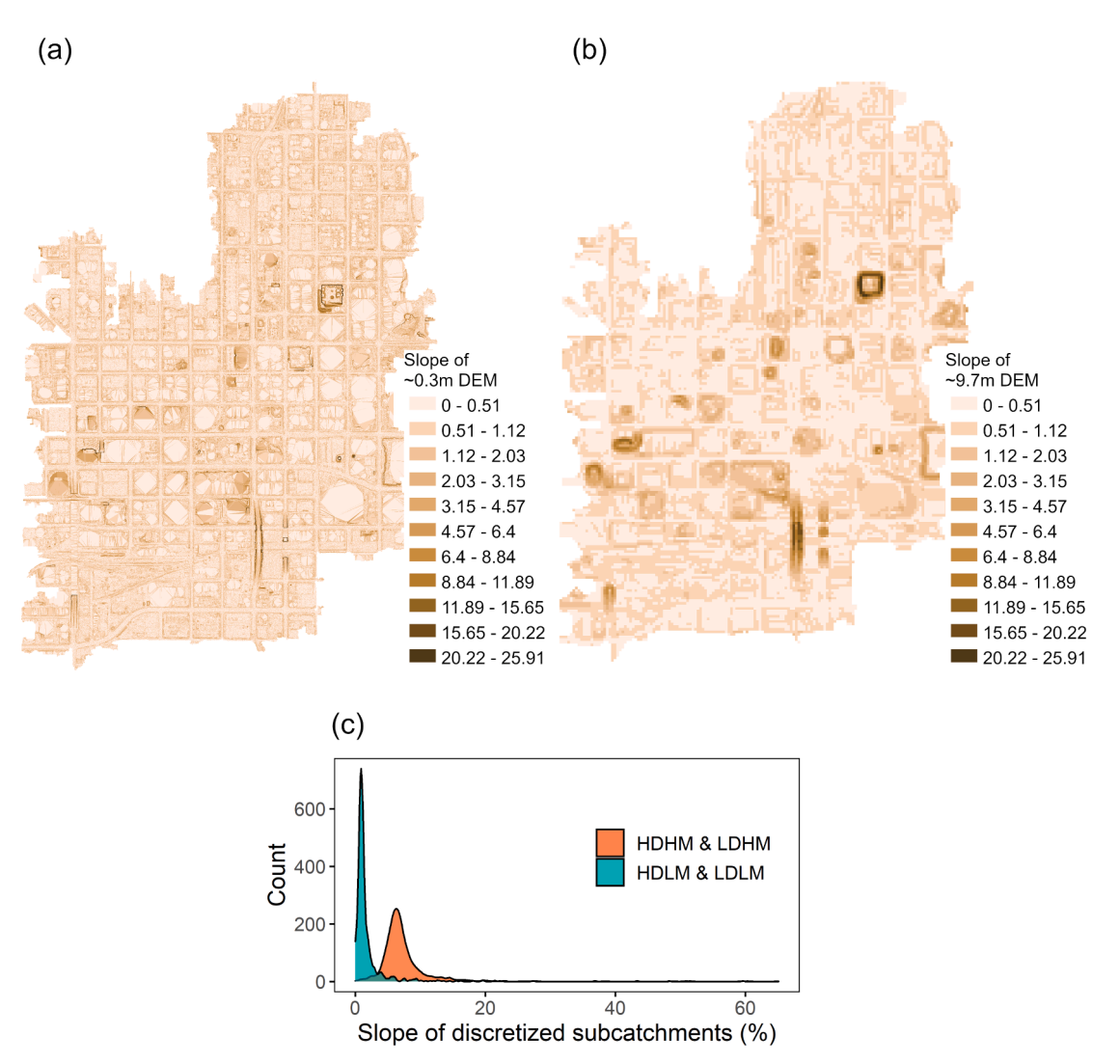


Fig. 7. Slope distributions of (a) high-resolution (0.3-m) DEM, (b) low-resolution (9.7-m) DEM and (c) sub catchments in high- and low-resolution models.

Fig. 7. It is notable that the slopes of low-resolution models (LDLM and HDLM) are much flatter than high-resolution models (LDHM and HDHM), which include details of street profile and curbs (Fig. 7c). This means that the heterogeneity of surface topography is well-captured by high-resolution models, whereas low-resolution models suffer a loss of terrain information (Fig. 7a, b).

Fig. 8 illustrates boxplots of maximum flood depth at each cell in the four sampling domains. HDLM has a narrower distribution, while LDHM has a wider distribution. The distributions for all four models are positively skewed. All interquartile ranges including maxima showed the similar pattern. LDHM resulted in the highest maximum flood depth (0.48 m), which is closest to the ground truth (i.e., HDHM) value of 0.45 m. Low-resolution models LDLM and HDLM underestimated maximum flood depth compared to the ground truth at 0.3 m and 0.28 m, respectively. Underestimation was most profound when the infrastructure data is complete, but model resolution is coarse (HDLM).

Fig. 9 illustrates the pluvial flooding fluxes in the four selective sampling models for all orifices that connect the coupled SWMM 1D's node with SWMM 2D's mesh grid cells. The flooding flux is the aggregate of all spatially distributed flood fluxes occurring at each timestep. All three tested model configurations overestimated the total flooding volume compared to the ground truth (HDHM). The overestimation of peak flooding flux was observed when there is incomplete data (LDHM and LDLM). This makes sense, as features such as inlets and conduits that would otherwise collect and convey stormwater are absent from these models. However, in the high-resolution model LDHM, the exchange of flood water between overland flow and underground drainage was more efficient compared to LDLM. Thus, compared with HDHM, LDHM may have incomplete data, but its higher resolution results in lower error than with LDLM in term of total flood volume.

The spatial flooding pattern of maximum grid cell flood depth for the four selective sampling models is shown in Fig. 10. The high flood depths occurred in HM models as highlighted in Box [I] (Fig. 10a,d), with the maximum occurring in LDHM (Fig. 10d), and the minimum occurred in HDLM (Fig. 10b). However, large flood extent occurred in LM models as highlighted in Box [II] (Fig. 10b,c), with the maximum occurring in HDLM, as compared to other two HM models. In the case of incomplete stormwater infrastructure data, missing features, particularly catch basins, preclude a realistic estimate of localized flooding and result in overestimates of flood volume, depth and extent. For example, as highlighted with Box [III] some of the areas flooded when infrastructure data is incomplete (LDLM and LDHM; Fig. 10c-d), remain dry when complete data is available (HDHM and HDLM; Fig. 10a-b). This is because in SWMM 1D-2D, overland flow drains to the underground

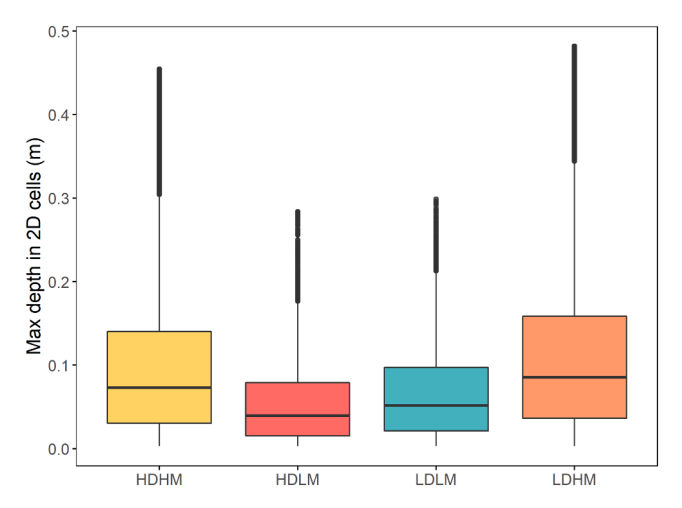


Fig. 8. Boxplots for distributions of maximum flooded depth in 2D grid cells. Note: Boxes represent the 25^{th} , 50^{th} and 75^{th} percentiles and whiskers represent \pm 1.5 \times IQR of the 25^{th} and 75^{th} percentiles.

drainage system through catch basins and can re-enter the drainage system after surcharge condition recedes. Note that this is a key distinction between SWMM 1D and SWMM 1D-2D. In SWMM 1D-2D, the exchange of flood water takes place between the surface and subsurface as the flux in flood volume changes, whereas in SWMM 1D, the water leaving the catch basins is counted as flooding and cannot reenter the drainage system. For this reason, the maximum system flooding simulated in the ground truth SWMM 1D model (89.6 $\rm m^3/s)$) is higher than in the two-dimensional HDHM model (73 $\rm m^3/s$). Also due to the limitations of the general 1D-2D modeling approach as employed in this study, where a larger portion of infrastructure data is missing such as an area highlighted in Box [IV], LD models will not estimate surface flooding, as all catchment areas must be linked to a catch basin.

Model resolution also plays a role, as overland flood water is more effective at re-entering the drainage system in higher-resolution models. The maximum depth out of the four selective sampling models was observed in the high-resolution models. However, the maximum flooded area and flood volume were observed in the low-resolution models, as local depressions are smoothed in the coarser DEM and the flood water spreads more readily to surrounding grid cells (Fig. 10). The error in flood depth, area and volume is the function of both the data completeness and model resolution. All surcharged flow spills onto the overland surface, represented by the mesh grid, and flows both on the surface in 2D and in through the pipe network in 1D. In the highresolution models, higher heterogeneity in elevation allows depressions to be better represented, so that there are chances for the surface flow to re-enter into the 1D components. This results in lower pluvial flood volume compared to the low-resolution models. It is crucial for mesh grids in SWMM 1D-2D to represent true topographic features at the scale of flooding hazards in order to model the physical process accurately. The use of 9.7 m DEM and 9.7 m mesh grids underestimates heterogeneity in surface elevation and topographic features relevant to pedestrian and vehicle flood hazards.

Fig. 11 summarizes the hydrological and hydraulic output for each scenario. In terms of hydrology, when the model resolution was coarse, infiltration and evaporation were slightly overestimated, and runoff was underestimated due to the flatter slopes and loss of terrain detail (Fig. 11). In term of hydraulics, in the 1D component of SWMM 1D-2D, the relative comparison of the total surcharged nodes showed higher number of nodes are surcharged in lower resolution model, this is because the rim elevation for nodes in HM and LM models are extracted from 0.3-m DEM with heterogeneous slope and 9.7-m DEM with flatter slope.

Our results agree with prior work by Ozdemir et al. (2013), which found an increase in maximum water depth and decrease in inundation extent with increasing DEM resolution. Prior work on DEM properties and flood inundation in natural stream reaches by Saksena and Merwade (2015) also found that coarser DEM resolution overpredicts the flood extent. Further, Hossain Anni et al (2020) used the 1D-2D coupled MIKE FLOOD model and found that the absence of detailed stormwater infrastructure data significantly overestimated flood water volume. Our work aligns with these results but extends this area of research to investigate how DEM resolution and data gaps interact (Fig. 11).

4.3. Research implications and limitations

Spatial data quality as defined by accuracy, current-ness, completeness, consistency (Fox et al., 1994), has been widely recognized to be of significant value in research and practice. This is especially true when electronic databases are produced, integrated and updated by multiple private and public sectors, and the reliance on secondary data sources increases for decision-support tools. As the effect of data completeness on urban flood modeling has not been fully understood, this study aimed to understand the effect of stormwater infrastructure data completeness on urban flood modeling. For the producers of these datasets, it is necessary to understand how incomplete data and errors propagate to

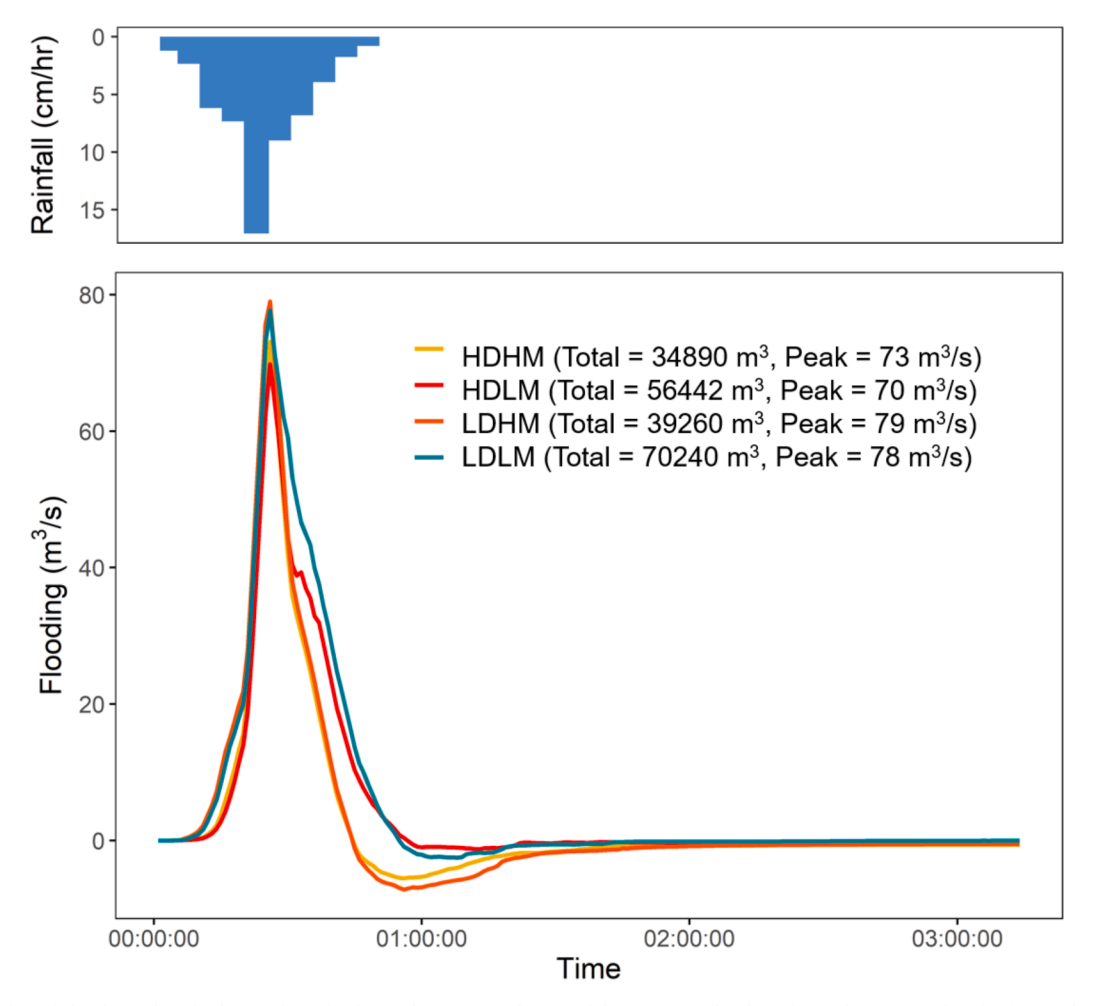


Fig. 9. Hyetograph and flooding (flux) hydrograph in the four selective sampling models. Negative flooding flux indicates net flow back into the drainage system. (For interpretation of the references to colour in this figure legend, the reader is referred to the web version of this article.)

model performance. As per Veregin (1999) data incompleteness occurs due to the errors of omission (i.e., infrastructure components not being recorded) and error of commission (i.e., assignment of incorrect data). For consumers of these datasets, this study cautions careful evaluation of data quality before analysis and decision making. The study also highlights the absence of a consistent approach to filling missing stormwater infrastructure data for modeling applications.

The first experiment of this study assessed the impact of stormwater infrastructure attribute-value completeness on hydrologic and hydrodynamic model performance by auto-filling data gaps using an algorithm based on available data and design standards. Note that there is no established way to fill missing data at scale, thus we have utilized design standards and available data that are readily available in practice and could be automated (as done here to facilitate Monte Carlo sampling) or executed manually (without the need for coding expertise). Therefore, the algorithm is appropriate to address a set of research questions closely linked to practice. Design standards vary locally, and the algorithms could be customized. For example, the minimum cover required for conduits differs regionally due to winter temperatures and risk of freezing. One limitation of this study is that the findings are specific to the city of Phoenix. The relationship between PMD, error and uncertainty might vary with the characteristics of the network and catchment. However, the method and algorithm could be readily adapted to other catchments to understand the effects of these characteristics. The error and precision resulting from missing data was in part a product of the algorithm used to estimate missing attribute-values. Further refinements to this algorithm could improve performance and reduce the error and

uncertainty associated with attribute–value gaps. Additionally, a limitation in random sampling was that the features were complete in all the models and only attribute-values get removed and replaced in sampling. The random sampling algorithm does not consider missing features, since it would require auto model building or network generating programming. This is out of scope of the current analysis but assessing the combined impact of missing feature and attribute-values is an important line of future work.

In addition to assessing the impact of missing attribute-values, the first experiment helps to prioritize data collection efforts. Results showed that missing attribute-values pertaining to the downstream region of the drainage network lead to higher model error and uncertainty when compared to upstream data gaps (Fig. 6). This suggests that, if resources for field surveys are limited, prioritizing the downstream section of the network would yield greater improvements in accuracy. Results also show that model performance is particularly sensitive to missing diameter values as shown by MAE and PBIAS (Tables 4 and 5). This suggests that efforts to improve attribute-value estimation algorithms should focus on diameter. However, the results presented here are for one catchment; testing the impact of the location of missing data in other catchments with different network geometry and topography should be explored further. Although the Monte Carlo based sampling algorithm was developed to investigate the effect of PMD and location of missing data on model performance, this experiment confirms the utility of the approach to filling missing attribute data. For example, the results demonstrate that missing roughness data could be effectively estimated using an empirical distribution of available roughness information, in

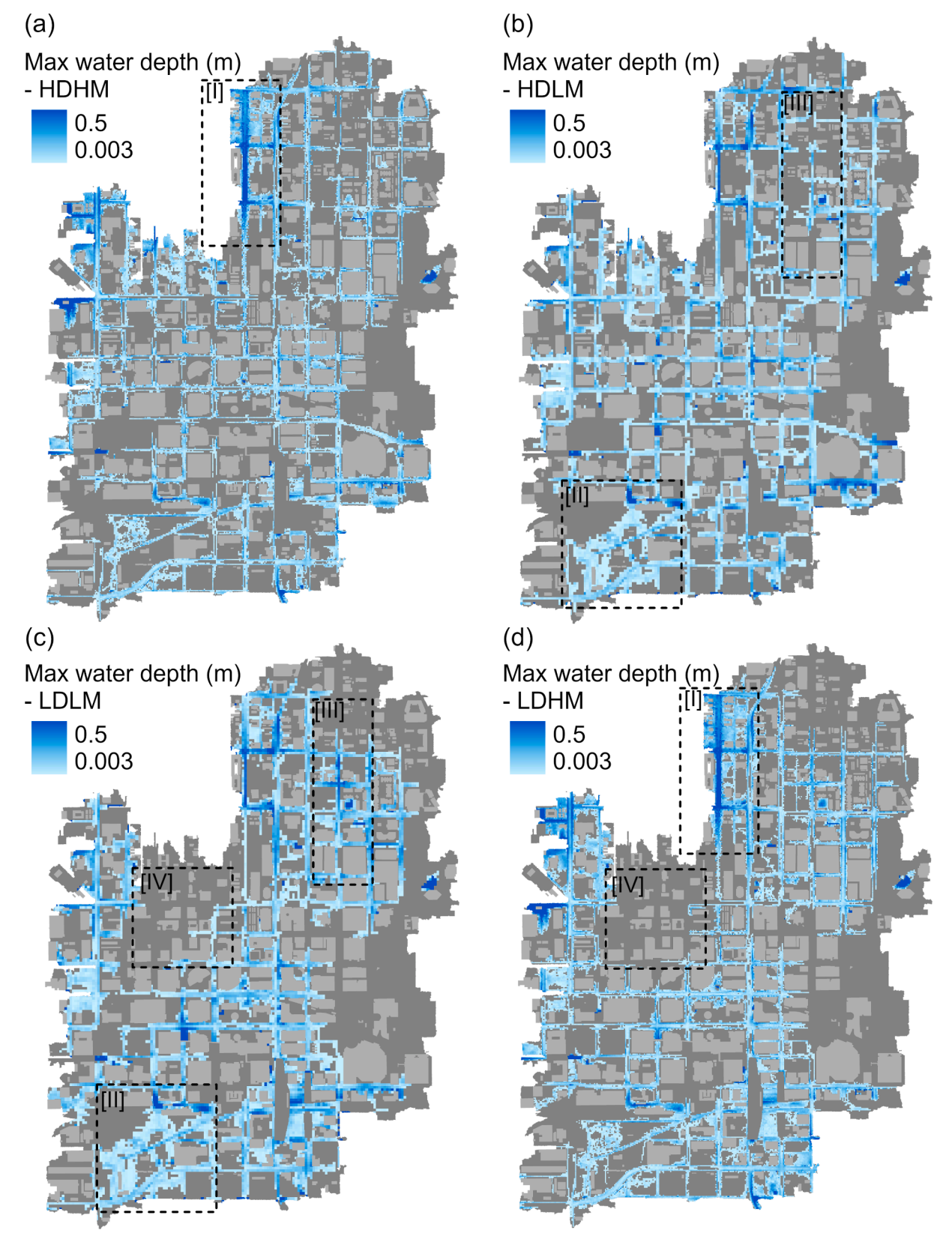


Fig. 10. Flooded extent and depth in four selective sampling models, (a) HDHM, (b) HDLM, (c) LDLM and (d) LDHM. Note: i). Peak flood depths are 0.45 m, 0.28 m, 0.3 m and 0.48 m for HDHM, HDLM, LDLM and LDHM, respectively, ii). Boxes [I - IV] are pointing to the differences in estimating depth and extent.

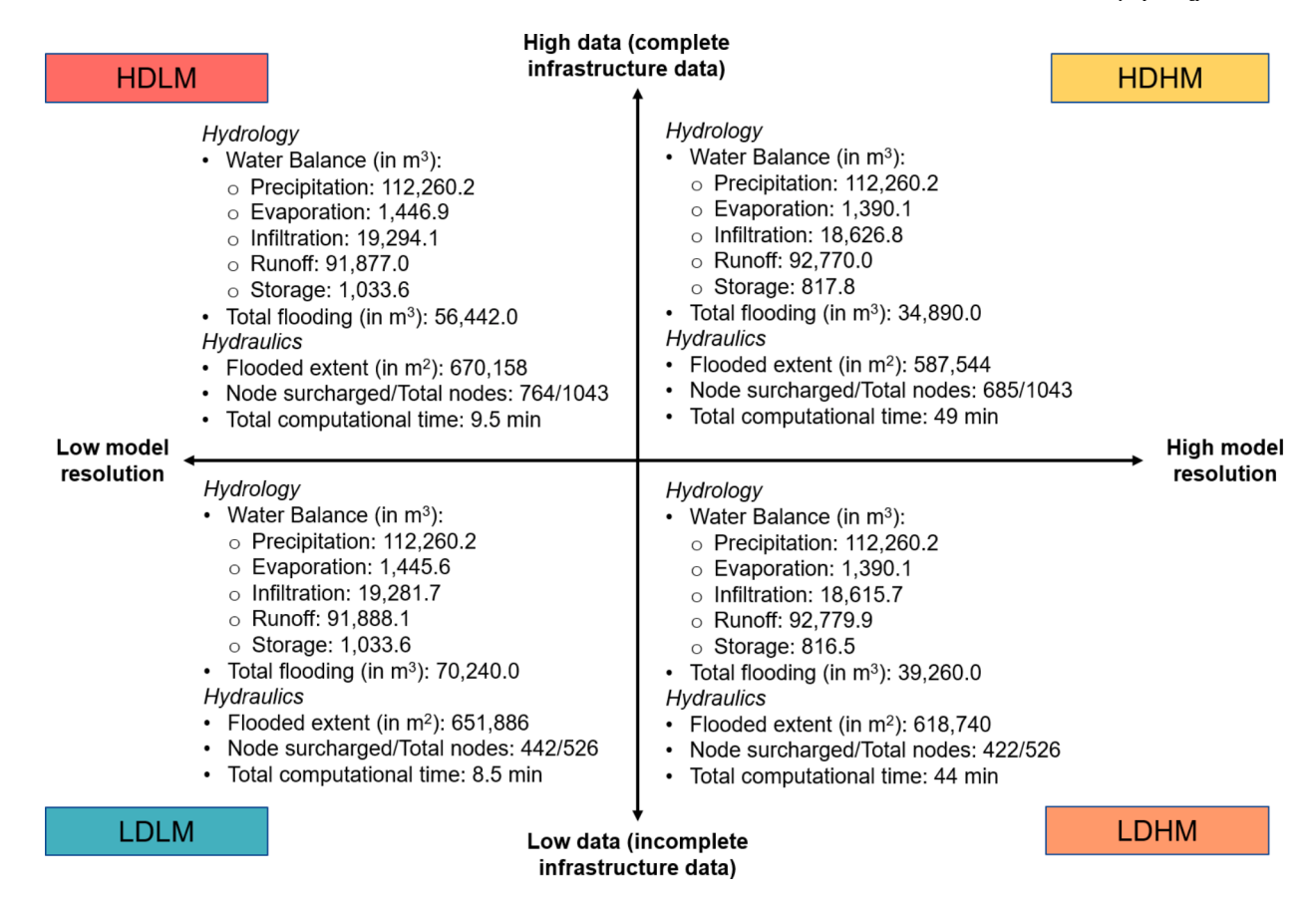


Fig. 11. Significance of data completeness and model resolution in terms of modeling hydrologic and hydraulic processes.

conjunction with information from adjacent conduits. Further improvements in estimating minimum depth and diameter when upstream or downstream attributes are missing, can improve the accuracy and precision of the model.

The second experiment of this study tested the effects of infrastructure data completeness and model resolution on model performance. Model resolution is usually selected based on the desired level of simulation accuracy, time availability and resource availability. Further analysis is needed to compare the value of incremental changes in model resolution to the effort and resources required. However, even when data and computational resources are readily available, the appropriate model resolution critically depends on the core purpose of the model. For example, within urban flood modeling, the core purpose of estimating total flood volume, versus the location or duration of flood impacts, might suggest a different model resolution. Low-resolution models have the benefit of lower computation time, which may be critical for applications such as real time pluvial flood forecasting or quick flood estimation. In this study, the low-resolution model simulation took 9.5 min while the high-resolution model took 49 min (note, these computation times were based on the computer specification of 64-bit i7 CPD @ 3.6 GHz processor used in this experiment). However, for infrastructure planning, including adaptation of existing stormwater infrastructure, model accuracy is more important than computation time. In pluvial flood estimation, the difference of a few inches of water could mean basement flooding, disruption of traffic and safety hazards. Further, the uncertainty from incomplete data and coarser model resolution selection is too high to optimize flood control measures such as green infrastructure, which have localized flood mitigation potential. We used 50 % missing features in the low data (incomplete infrastructure data) models and further analysis using different levels of missing stormwater infrastructure features, in combination with different model resolutions on different types of catchments would be beneficial. While the key effects quantified here are specific to the study area some results are generalizable as there will be similar but varied degree of error, bias and uncertainty in simulating hydrologic-hydraulic variables due to missing attribute-values and features data of stormwater infrastructure, and improper selection of model resolution.

5. Conclusions

This study consists of a two-part experiment to investigate the effect of data completeness and model resolution on urban flood model performance by random sampling and selective sampling. An algorithm was built to randomly remove and replace attribute-values for the hydrologic-hydraulic stormwater model built using the EPA's SWMM. Random sampling was done for attribute-values using the 1D model; then, selective sampling was applied to feature data completeness and model resolution using the computationally demanding 1D-2D model. Results demonstrated that the relationship between model uncertainty and PMD is dependent on the attribute or parameter in question. In contrast, accuracy consistently decreases with an increasing PMD, except for diameter. We also found that missing data in the downstream section of the catchment leads to greater uncertainty and lower accuracy compared to missing data upstream. This finding can inform the prioritization of data collection and verification efforts where resources are limited. The total flood duration and extent may be over or underestimated due to incomplete infrastructure data, depending on model resolution. In the SWMM 1D-2D selective sampling, the highest flood depth was simulated by the high-resolution models. In contrast, the highest flood extent and volume were simulated by the low-resolution models. In sum, both data completeness and model resolution determine the accuracy of flood depth, extent and volume estimates. This emphasizes the importance of high-resolution modeling and complete data for urban flood estimation at the scale of pedestrian and vehicle

A. Shrestha et al. Journal of Hydrology 607 (2022) 127498

flood hazards where accurate flood extent, volume and depth are critical.

The risks of pluvial flooding are projected to grow in many cities as they experience more intense precipitation due to climate change and as urbanization decreases permeable area. Modeling can be an effective tool to understand pluvial flooding and make projections that enable effective adaptation and response. Understanding, quantifying and communicating error and uncertainties arising from various sources are essential for decision making. However, infrastructure data gaps are a common obstacle and prior research has not addressed the impact of these gaps on model performance. In addition, access to high-resolution LiDAR is limited globally. In this study we focused on infrastructure data gap and model resolution, which are key pieces to an accurate and precise model. This study shows that the error and uncertainty in simulating hydrologic-hydraulic variables due to prevalence of missing stormwater infrastructure data, and selection of improper model resolution could be significant and might affect the quality of the model application. Hydrologic-hydraulic models are increasingly being used in stormwater design, real time modeling of pluvial flooding, and impact or damage assessment. With the growing focus on the importance of pluvial flooding as well as increasing use of physically based models we need a cost-effective approach to overcome data gaps. This problem can be dissected into two sub parts: assessment and application. The Monte Carlo based sampling algorithm was developed as an assessment approach to quantify the effect of missing attribute-value. As presented here, the algorithm can also be used to fill missing attribute-values in large stormwater infrastructure datasets. It can be further developed to improve its accuracy and precision and to adapt it to different contexts. In sum, this work takes a first step to address an understudied challenge in urban stormwater modeling, developing tools and insights useful in both research and practice.

CRediT authorship contribution statement

Ashish Shrestha: Conceptualization, Methodology, Data Curation, Investigation, Software, Formal analysis, Validation, Visualization, Writing - original draft, Writing - review & editing. Giuseppe Mascaro: Supervision, Writing - review & editing. Margaret Garcia: Conceptualization, Methodology, Supervision, Resources, Funding acquisition, Writing - review & editing.

Declaration of Competing Interest

The authors declare that they have no known competing financial interests or personal relationships that could have appeared to influence the work reported in this paper.

Acknowledgements

This work is supported by National Science Foundation (NSF) Smart and Connected Communities Program (1831475). The data for analysis and model building had been provided by Phoenix Public Works Department and Flood Control District of Maricopa County.

Appendix A. Supplementary data

Supplementary data to this article can be found online at https://doi.org/10.1016/j.jhydrol.2022.127498.

References

- ADOT, 2014. Highway Drainage Design Manual Volume 2 Hydrology. Arizona Department of Transportation 206 S. 17th Ave, Phoenix, AZ 85007.
- American Society of Civil Engineers, 1992. Design and construction of urban stormwater management systems, American Society of Civil Engineers, Manuals and Reports on Engineering Practice. https://doi.org/10.1061/9780872628557.

Arrighi, C., Campo, L., 2019. Effects of digital terrain model uncertainties on highresolution urban flood damage assessment. J. Flood Risk Manage. 12, 1–12. https://

- ASFPM, 2020. Urban Flood Hazards: Challenges and Opportunities. Association of State Floodplain Managers, Stormwater Management Committee, 8301 Excelsior Dr., Madison, WI 53717.
- ASU, 2018. Metro Phoenix USGS LiDAR Data [WWW Document]. URL: https://lib.asu.edu/geo.
- Balling, R.C., Brazel, S.W., 1987. Diurnal Variations in Arizona Monsoon Precipitation Frequencies. Mon. Wea. Rev. 115 (1), 342–346.
- Bates, P.D., Marks, K.J., Horritt, M.S., 2003. Optimal use of high-resolution topographic data in flood inundation models. Hydrol. Process. 17 (3), 537–557. https://doi.org/ 10.1002/hyp.1113.
- Bermúdez, M., Zischg, A.P., 2018. Sensitivity of flood loss estimates to building representation and flow depth attribution methods in micro-scale flood modelling. Nat. Hazards 92 (3), 1633–1648. https://doi.org/10.1007/s11069-018-3270-7.
- Bitew, M.M., Gebremichael, M., 2011. Evaluation of satellite rainfall products through hydrologic simulation in a fully distributed hydrologic model. Water Resour. Res. 47, 1–11. https://doi.org/10.1029/2010WR009917.
- Cantone, J., Schmidt, A., 2011. Improved understanding and prediction of the hydrologic response of highly urbanized catchments through development of the Illinois Urban Hydrologic Model. Water Resour. Res. 47, 1–16. https://doi.org/10.1029/2010WR009330
- Chang, T.J., Wang, C.H., Chen, A.S., 2015. A novel approach to model dynamic flow interactions between storm sewer system and overland surface for different land covers in urban areas. J. Hydrol. 524, 662–679. https://doi.org/10.1016/j. ihydrol.2015.03.014.
- Chow, V. Te, Maidment, D.R., Mays, L.W., 1998. Applied Hydrology.
- City of Phoenix, 2013. Storm Water Policies and Standards.
- Dawson, R.J., Speight, L., Hall, J.W., Djordjevic, S., Savic, D., Leandro, J., 2008. Attribution of flood risk in urban areas. J. Hydroinformatics 10, 275–288.
- Dottori, F., Di Baldassarre, G., Todini, E., 2013. Detailed data is welcome, but with a pinch of salt: Accuracy, precision, and uncertainty in flood inundation modeling. Water Resour. Res. 49 (9), 6079–6085. https://doi.org/10.1002/wrcr.20406.
- Elliott, A.H., Trowsdale, S.A., Wadhwa, S., 2009. Effect of Aggregation of On-Site Storm-Water Control Devices in an Urban Catchment Model. J. Hydrol. Eng. 14 (9), 975–983. https://doi.org/10.1061/(ASCE)HE.1943-5584.0000064.
- Farris, S., Deidda, R., Viola, F., Mascaro, G., 2021. On the Role of Serial Correlation and Field Significance in Detecting Changes in Extreme Precipitation Frequency. Water Resour. Res. 57 (11).
- Festing, H., Copp, C., Sprague, H., Wolf, D., Shorofsky, B., Nichols, K., 2014. The Prevalence and Cost of Urban Flooding: A Case Study of Cook County, IL.
- Fewtrell, T.J., Bates, P., Horritt, M., Hunter, N.M., 2008. Evaluating the effect of scale in flood inundation modelling in urban environments. Hydrol. Process. 22, 5107–5118. https://doi.org/10.1002/hyp.
- Fewtrell, T.J., Duncan, A., Sampson, C.C., Neal, J.C., Bates, P.D., 2011. Benchmarking urban flood models of varying complexity and scale using high resolution terrestrial LiDAR data. Phys. Chem. Earth. 36 (7-8), 281–291.
- Finney, K., Gharabaghi, B., 2011. Using the PCSWMM 2010 SRTC Tool to Design a Compost Biofilter for Highway Stormwater Runoff Treatment. J. Water Manag. Model. 6062, 157–166. https://doi.org/10.14796/jwmm.r241-09.
- Finney, K., James, R., Perera, N., 2012. Benchmarking SWMM5/PCSWMM 2D Model Performance, in: International Conference on Water Management Modeling. ON. First Street Foundation, 2020. The First National Flood Risk Assessment. Defining America's Growing Risk 1–163.
- Fox, C., Levitin, A., Redman, T., 1994. The notion of data and its quality dimensions. Inf. Process. Manag. 30 (1), 9–19. https://doi.org/10.1016/0306-4573(94)90020-5. Gallegos, H.A., Schubert, J.E., Sanders, B.F., 2009. Two-dimensional, high-resolution
- Gallegos, H.A., Schubert, J.E., Sanders, B.F., 2009. Two-dimensional, high-resolution modeling of urban dam-break flooding: A case study of Baldwin Hills. California. Adv. Water Resour. 32 (8), 1323–1335. https://doi.org/10.1016/j. advwatres.2009.05.008.
- Guo, K., Guan, M., Yu, D., 2020. Urban surface water flood modelling a comprehensive review of current models and future challenges. Hydrol. Earth Syst. Sci. Discuss. 1–27 https://doi.org/10.5194/hess-2020-655.
- Raines, G.L., 1997. Elements of spatial data quality. Comput. Geosci. 23 (1), 135.
- Hall, J.W., Sayers, P.B., Dawson, R.J., 2005. National-scale assessment of current and future flood risk in England and Wales. Nat. Hazards 36 (1-2), 147–164. https://doi. org/10.1007/s11069-004-4546-7.
- Harvey, R., de Lange, M., McBean, E., Trenouth, W., Singh, A., James, P., 2017. Asset condition assessment of municipal drinking water, wastewater and stormwater systems-Challenges and directions forward. Can. Water Resour. J. 42 (2), 138–148. https://doi.org/10.1080/07011784.2016.1224684.
- Henonin, J., Russo, B., Mark, O., Gourbesville, P., 2013. Real-time urban flood forecasting and modelling - A state of the art. J. Hydroinformatics 15, 717–736. https://doi.org/10.2166/hydro.2013.132.
- Hjelmstad, A., Shrestha, A., Garcia, M., Mascaro, G., 2021. Propagation of radar rainfall uncertainties into urban pluvial flood modeling during the North American monsoon. Hydrol. Sci. J. 66 (15), 2232–2248. https://doi.org/10.1080/ 02626667.2021.1980216.
- Hossain Anni, A., Cohen, S., Praskievicz, S., 2020. Sensitivity of urban flood simulations to stormwater infrastructure and soil infiltration. J. Hydrol. 588, 125028. https:// doi.org/10.1016/j.jhydrol.2020.125028.
- James, R., Finney, K., Perera, N., James, B., Peyron, N., 2013. SWMM5/PCSWMM Integrated 1D-2D Modeling, in: A.S. Donigian, AQUA TERRA Consultants; Richard Field, U.E. (retired); M.B.J. (Ed.), Fifty Years Of Watershed Modeling - Past, Present And Future. ECI Symposium Series. http://dc.engconfintl.org/watershed/12.

- James, W., 2003. Rules for responsible modeling. Guelph, Ontario: CHI.
- James, W., Rossman, L.A., James, W.R.C., 2010. User's guide to SWMM5 13th Edition. Jiang, Y., Zevenbergen, C., Ma, Y., 2018. Urban pluvial flooding and stormwater management: A contemporary review of China's challenges and "sponge cities" strategy. Environ. Sci. Policy 80, 132–143. https://doi.org/10.1016/j. envsci.2017.11.016.
- Jung, I.W., Chang, H., Moradkhani, H., 2011. Quantifying uncertainty in urban flooding analysis considering hydro-climatic projection and urban development effects. Hydrol. Earth Syst. Sci. 15, 617–633. https://doi.org/10.5194/hess-15-617-2011.
- Kabisch, N., Korn, H., Stadler, J., Bonn, A., 2017. Nature-based solutions to climate change adaptation in urban areas: Linkages between science. policy and practice. Springer Nature
- Krebs, G., Kokkonen, T., Valtanen, M., Setälä, H., Koivusalo, H., 2014. Spatial resolution considerations for urban hydrological modelling. J. Hydrol. 512, 482–497. https://doi.org/10.1016/j.jhydrol.2014.03.013.
- Kuriqi, A., Hysa, A., 2021. Multidimensional Aspects of Floods: Nature-Based Mitigation Measures from Basin to River Reach Scale. Springer, Berlin Heidelberg, Berlin, Heidelberg, pp. 1–23.
- Leandro, J., Chen, A.S., Djordjević, S., Savić, D.A., 2009. Comparison of 1D/1D and 1D/2D coupled (sewer/surface) hydraulic models for urban flood simulation. J. Hydraul. Eng. 135 (6), 495–504. https://doi.org/10.1061/(ASCE)HY.1943-7900.0000037.
- Leandro, J., Martins, R., 2016. A methodology for linking 2D overland flow models with the sewer network model SWMM 5.1 based on dynamic link libraries. Water Sci. Technol. 73, 3017–3026. https://doi.org/10.2166/wst.2016.171.
- Leitão, J.P., Boonya-aroonnet, S., Prodanović, D., Maksimović, Č., 2009. The influence of digital elevation model resolution on overland flow networks for modelling urban pluvial flooding. Water Sci. Technol. 60, 3137–3149. https://doi.org/10.2166/ wst 2009 754
- Leitão, J.P., Moy de Vitry, M., Scheidegger, A., Rieckermann, J., 2016. Assessing the quality of digital elevation models obtained from mini unmanned aerial vehicles for overland flow modelling in urban areas. Hydrol. Earth Syst. Sci. 20 (4), 1637–1653. https://doi.org/10.5194/hess-20-1637-201610.5194/hess-20-1637-2016supplement.
- Leitão, J.P., de Sousa, L.M., 2018. Towards the optimal fusion of high-resolution Digital Elevation Models for detailed urban flood assessment. J. Hydrol. 561, 651–661. https://doi.org/10.1016/j.jhydrol.2018.04.043.
- Leitold, R., Garschagen, M., Tran, V., Revilla Diez, J., 2021. Flood risk reduction and climate change adaptation of manufacturing firms: Global knowledge gaps and lessons from Ho Chi Minh City. Int. J. Disaster Risk Reduct. 61, 102351. https://doi. org/10.1016/j.ijdrr.2021.102351.
- Leutnant, D., Döring, A., Uhl, M., 2019. swmmr an R package to interface SWMM. Urban Water J. 16 (1), 68–76. https://doi.org/10.1080/1573062X.2019.1611889
- Lyu, H., Ni, G., Cao, X., Ma, Y.u., Tian, F., 2018. Effect of temporal resolution of rainfall on simulation of urban flood processes. Water (Switzerland) 10 (7), 880. https://doi. org/10.3390/w10070880.
- Martínez, C., Sanchez, A., Toloh, B., Vojinovic, Z., 2018. Multi-objective Evaluation of Urban Drainage Networks Using a 1D/2D Flood Inundation Model. Water Resour. Manag. 32 (13), 4329–4343. https://doi.org/10.1007/s11269-018-2054-x.
- Mascaro, G., 2020. Comparison of Local, Regional, and Scaling Models for Rainfall Intensity–Duration–Frequency Analysis. J. Appl. Meteorol. Climatol. 59, 1519–1536. https://doi.org/10.1175/JAMC-D-20-0094.1.
- Mascaro, G., 2018. On the distributions of annual and seasonal daily rainfall extremes in central Arizona and their spatial variability. J. Hydrol. 559, 266–281. https://doi. org/10.1016/j.jhydrol.2018.02.011.
- Mascaro, G., 2017. Multiscale spatial and temporal statistical properties of rainfall in central Arizona. J. Hydrometeorol. 18, 227–245. https://doi.org/10.1175/JHM-D
- Moftakhari, H.R., AghaKouchak, A., Sanders, B.F., Feldman, D.L., Sweet, W., Matthew, R. A., Luke, A., 2015. Increased nuisance flooding due to sea-level rise: past and future. Geophys. Res. Lett. 42, 9846–9852. https://doi.org/10.1002/2015GL066072.
- MRLC, n.d. Urban Imperviousness [WWW Document]. Multi-Resolution L. Charactieristics Consortium, Natl. L. Cover Database. URL https://www.mrlc.gov/data.
- Nanía, L.S., León, A.S., García, M.H., 2015. Hydrologic-Hydraulic Model for Simulating Dual Drainage and Flooding in Urban Areas: Application to a Catchment in the Metropolitan Area of Chicago. J. Hydrol. Eng. 20 (5), 04014071.
- Nithila Devi, N., Sridharan, B., Kuiry, S.N., 2019. Impact of urban sprawl on future flooding in Chennai city. India. J. Hydrol. 574, 486–496. https://doi.org/10.1016/j. jhydrol.2019.04.041.
- NOAA/NWS, n.d. NOAA Atlas 14 Point Precipitation Frequency Estimates: KS [WWW Document]. NOAA's Natl. Weather Serv. Hydrometeorol. Des. Stud. Cent. URL https://hdsc.nws.noaa.gov/hdsc/pfds/pfds_map_cont.html.
- Noh, S.J., Lee, J.H., Lee, S., Kawaike, K., Seo, D.J., 2018. Hyper-resolution 1D–2D urban flood modelling using LiDAR data and hybrid parallelization. Environ. Model. Softw. 103, 131–145. https://doi.org/10.1016/j.envsoft.2018.02.008.
- NWS, 2014. Record rainfall & widespread flooding across Phoenix Metro Area [WWW Document]. NOAA's Natl, Weather Serv https://www.wrh.noaa.gov/psr/pns/2014/September/Sep8Flooding.php.

- NWS, n.d. Turn Around Don't Drown [WWW Document]. URL https://www.weather.gov/tsa/hydro tadd.
- Ozdemir, H., Sampson, C.C., De Almeida, G.A.M., Bates, P.D., 2013. Evaluating scale and roughness effects in urban flood modelling using terrestrial LIDAR data. Hydrol. Earth Syst. Sci. 17, 4015–4030. https://doi.org/10.5194/hess-17-4015-2013.
- Pathak, C.S., Teegavarapu, R.S.V., Olson, C., Singh, A., Lal, A.M.W., Polatel, C., Zahraeifard, V., Senarath, S.U.S., 2015. Uncertainty Analyses in Hydrologic/ Hydraulic Modeling: Challenges and Proposed Resolutions. J. Hydrol. Eng. 20 (10), 02515003
- Prokić, M., Savić, S., Pavić, D., 2019. Pluvial flooding in Urban Areas Across the European Continent. Geogr. Pannonica 23 (4), 216–232. https://doi.org/10.5937/gp.23-23508
- Rahmati, O., Darabi, H., Panahi, M., Kalantari, Z., Naghibi, S.A., Ferreira, C.S.S., Kornejady, A., Karimidastenaei, Z., Mohammadi, F., Stefanidis, S., Tien Bui, D., Haghighi, A.T., 2020. Development of novel hybridized models for urban flood susceptibility mapping. Sci. Rep. 10 (1) https://doi.org/10.1038/s41598-020-69703-7
- Rosenzweig, B.R., McPhillips, L., Chang, H., Cheng, C., Welty, C., Matsler, M., Iwaniec, D., Davidson, C.I., 2018. Pluvial flood risk and opportunities for resilience. Wiley Interdiscip. Rev. Water 5, 1–18. https://doi.org/10.1002/wat2.1302.
- Rossman, L.A., 2017. Storm Water Management Model Reference Manual Volume II Hydraulics. Office of Research and Development, U.S. Environmental Protection Agency, Cincinnati, OH. https://doi.org/10.1056/NEJMra0804615.
- Rossman, L.A., 2006. Storm Water Management Model Quality assurance report:
 Dynamic Wave Flow Routing. United States Environmental Protection Agency,
 Cincinnati, OH.
- Saksena, S., Merwade, V., 2015. Incorporating the effect of DEM resolution and accuracy for improved flood inundation mapping. J. Hydrol. 530, 180–194. https://doi.org/ 10.1016/j.jhydrol.2015.09.069.
- Sampson, C.C., Fewtrell, T.J., Duncan, A., Shaad, K., Horritt, M.S., Bates, P.D., 2012. Use of terrestrial laser scanning data to drive decimetric resolution urban inundation models. Adv. Water Resour. 41, 1–17. https://doi.org/10.1016/j. advwatres.2012.02.010.
- Seyoum, S.D., Vojinovic, Z., Price, R.K., Weesakul, S., 2012. Coupled 1D and Noninertia 2D Flood Inundation Model for Simulation of Urban Flooding. J. Hydraul. Eng. 138 (1), 23–34.
- Sharif, H.O., Ogden, F.L., Krajewski, W.F., Xue, M., 2002. Numerical simulations of radar rainfall error propagation. Water Resour. Res. 38 (8), 15-1–15-14.
- Sheppard, P.R., Comrie, A.C., Packin, G.D., Angersbach, K., Hughes, M.K., 2002. The climate of the US Southwest. Clim. Res. 21 (3), 219–238.
- Tanaka, T., Kiyohara, K., Tachikawa, Y., 2020. Comparison of fluvial and pluvial flood risk curves in urban cities derived from a large ensemble climate simulation dataset: A case study in Nagoya. Japan. J. Hydrol. 584, 124706. https://doi.org/10.1016/j. ibydrol.2020.124706.
- The National Academy Press, 2019. Framing the challenge of urban flooding in the United States. Washington DC.
- University of Maryland, Center for Disaster Resilience, and Texas A&M University, Galveston Campus, Center for Texas Beaches and Shores. The Growing Threat of Urban Flooding: A National Challenge. 2018. College Park: A. James Clark School of Engineering.
- USDA-NRCS, n.d. Web Soil Survey [WWW Document]. United States Dep. Agric. Nat. Resour. Conserv. Serv. URL https://websoilsurvey.sc.egov.usda.gov/App/WebSoilSurvey.acgv.
- USGS, n.d. 3D Elevation Program (3DEP) [WWW Document]. URL https://www.usgs.go v/core-science-systems/ngp/3dep/about-3dep-products-services?qt-science_suppo rt page related con=0#qt-science support page related con.
- Veregin, H., 1999. Data quality parameters, in: Geographical Information Systems. pp. 177–189.
- Vojinovic, Z., Tutulic, D., 2009. On the use of 1D and coupled 1D–2D modelling approaches for assessment of flood damage in urban areas. Urban Water J. 6 (3), 183–199. https://doi.org/10.1080/15730620802566877.
- Wehner, M.F., Arnold, J.R., Knutson, T., Kunkel, K.E., LeGrande, A.N., 2017. Ch. 8: Droughts, Floods, and Wildfires. Climate Science Special Report: Fourth National Climate Assessment, Volume I, Climate Science Special Report: Fourth National Climate Assessment, Volume I. Washington, DC. https://doi.org/10.7930/ J0CJ8BNN.
- Wickham, H., 2009. ggplot2, Applied Spatial Data Analysis with R. Springer New York, New York, NY. https://doi.org/10.1007/978-0-387-98141-3.
- $\label{lem:west.} WRCC, n.d. \ Evaporation \ stations \ [WWW Document]. \ West. \ Reg. \ Clim. \ Cent. \ URL \ https://wrcc.dri.edu/Climate/comp_table_show.php?stype=pan_evap_avg.$
- Wu, X., Wang, Z., Guo, S., Lai, C., Chen, X., 2018. A simplified approach for flood modeling in urban environments. Hydrol. Res. 49, 1804–1816. https://doi.org/ 10.2166/nh.2018.149.
- Zhang, W., Villarini, G., Vecchi, G.A., Smith, J.A., 2018. Urbanization exacerbated the rainfall and flooding caused by hurricane Harvey in Houston. Nature 563 (7731), 384–388. https://doi.org/10.1038/s41586-018-0676-z.